SYNGAS PRODUCTION BY DRY REFORMING OF METHANE: THERMODYNAMIC AND MODELING STUDY

A DISSERTATION

Submitted in partial fulfillment of the
requirements for the award of the degree
of
MASTER OF TECHNOLOGY
in
CHEMICAL ENGINEERING
(With Specialization in Computer Aided Process Plant Design)

By

FAYIZA YAQUB

DEPARTMENT OF CHEMICAL ENGINEERING
INDIAN INSTITUTE OF TECHNOLOGY ROORKEE
ROORKEE-247 667 (INDIA)
JUNE, 2013

DECLARATION

I hereby assure that the work presented in this dissertation entitled **"Syngas Production By Dry Reforming of Methane: Thermodynamic and Modeling Study"** is submitted in partial fulfilment of the requirement for the award of the degree of Masters of Technology in Chemical Engineering with the specialization in Computer Aided Process Plant Design (CAPPD) at the Indian Institute of Technology Roorkee, is an authentic record of my original work carried out under the guidance of **Dr. (Mrs) Shashi**, Associate Professor. I have not submitted the matter embodied in this dissertation for the award of any other degree.

Fayiza.

Fayiza Yaqub

Place: Roorkee

Date: 13th June, 2013

CERTIFICATE

This is to certify that Ms. Fayiza Yaqub has completed the dissertation entitled **"Syngas Production By Dry Reforming of Methane: Thermodynamic and Modeling Study"** under my supervision. This is to certify that the above statement made by the candidate is correct to the best of my knowledge.

Shashi 10/6/13

Dr. Shashi

Associate Professor,

Department of Chemical Engineering

Indian Institute of Technology, Roorkee

ACKNOWLEDGEMENT

It is with a deep sense of gratitude that I profoundly acknowledge my indebtness to my supervisor, **Dr. (Mrs) Shashi**, Associate Professor, Chemical Engineering Department for her perceptive suggestions and comments that helped me to remain motivated and enthused in compiling this work. My special thanks are due to Dr. Surendar Kumar, Professor, Chemical Engineering Department for his inspiring guidance. His infallible supervision and guidance has made this work a more rewarding experience for me.

Last but not the least, it is all owed to the blessings of my parents which helped me to complete the work in due time

Fayiza.

Fayiza Yaqub

ABSTRACT

Carbon dioxide reforming of methane produces synthesis gas with low hydrogen to carbon monoxide ratio, which is desirable for many industrial synthesis processes. This reaction also has very important environmental implications since both methane and carbon dioxide contribute to the greenhouse effect. Converting these gases into a valuable feedstock may significantly reduce the atmospheric emissions of CO_2 and CH_4.The dry reforming is carried out with excess CO_2 to promote reverse water gas shift reaction (RWGS) which results in lower H_2/CO ratio. Carbon deposition causing catalyst deactivation is the major problem inhibiting the industrial application of the dry reforming reaction. Thermodynamically, the most probable reactions leading to carbon formation during dry reforming are methane cracking, boudouard reaction, CO reduction and CO_2 reduction reactions. All the four carbon forming reactions are employed to examine the thermodynamic possibility of carbon formation and thermodynamic equilibrium calculations have been performed with Aspen plus based on direct minimization of Gibbs free energy method. The effects of CO_2/CH_4 ratio (1–3), reaction temperature (873–1500 K) and hydrogen addition (0-10%) at 1atm pressure on equilibrium conversions, product compositions and solid carbon were studied. On the basis of thermodynamic analysis the optimal working conditions for syngas having H_2/CO ratio of 1 with negligible amount of carbon formation were obtained and were used to simulate the performance of four reactors, two fixed beds (FBR1 & FBR2) and two membrane reactors (MR1 &MR2) in terms of CH_4 conversion, H_2/CO ratio and yield of H_2.

For this purpose a comprehensive, steady state, one dimensional, isothermal mathematical model equations for dry reforming reactions in membrane and fixed bed reactor have been developed. Two types of catalysts have been used in the study: Rh/Al_2O_3 and Ni/Al_2O_3. The axial and the radial dispersion in the model are assumed to be negligible and the external mass transfer resistance in the catalyst bed is also neglected. The model equations developed have been solved by ODE solver tool in MATLAB. The reactors FBR1 and MR1 that were packed with Rh/Al_2O_3 catalyst gave higher CH_4 conversion as compared to FBR2 and MR2 that were packed with Ni/Al_2O_3. Also, membrane reactors MR1 and MR2 have been found to provide better performance as compared to fixed bed reactor FBR1 and FBR2 respectively.

CONTENTS

LIST OF FIGURES

LIST OF TABLES

NOMENCLATURE

A_0	Pre exponential factor (mol $m^{-2}s^{-1}Pa^{-0.5}$)
D_i	effective permeability of species i (mol $m^{-2}Pa^{-1}s^{-1}$)
E_a	Activation energy (kJ/mol)
F_{sCH4}	molar flow rate of methane at outlet of reactor on the shell side. (μmol/s)
F_{sCO}	molar flow rate of carbon monoxide at outlet of reactor on the shell side. (μmol/s)
F_{sCO2}	molar flow rate of carbon dioxide at outlet of reactor on the shell side. (μmol/s)
F_{sH2}	molar flow rate of hydrogen at outlet of reactor on the shell side. (μmol/s)
F_{sH2O}	molar flow rate of water at outlet of reactor on the shell side. (μmol/s)
F^0_{sN2}	molar flow rate of nitrogen at inlet of reactor on the shell side. (μmol/s)
F_{si}	molar flow rate of i^{th} component at outlet of reactor on the shell side. (μmol/s)
F^0_{si}	molar flow rate of i^{th} component at inlet of reactor on the shell side. (μmol/s)
F_{tCH4}	molar flow rate of methane component at outlet of reactor on the tube side. (μmol/s)
F^0_{tCH4}	molar flow rate of methane at inlet of reactor on the tube side. (μmol/s)
F_{tCO}	molar flow rate of carbon dioxide at outlet of reactor on the tube side. (μmol/s)
F_{tCO2}	molar flow rate of carbon dioxide at outlet of reactor on the tube side. (μmol/s)
F_{tH2}	molar flow rate of hydrogen at outlet of reactor on the tube side. (μmol/s)
F_{tH2O}	molar flow rate of water at outlet of reactor on the tube side. (μmol/s)
F_{tN2}	molar flow rate of nitrogen at outlet of reactor on the tube side. (μmol/s)
F_{ti}	molar flow rate of i^{th} component at outlet of reactor on the tube side. (μmol/s)
F^0_{ti}	molar flow rate of i^{th} component at inlet of reactor on the tube side. (μmol/s)
K_{CH4}	adsorption equilibrium constant of CH_4 (atm^{-1})
K_{CO2}	adsorption equilibrium constant of CO_2 (atm^{-1})
P_{sT}	total pressure of component i in shell side (atm)
P_{si}	partial pressure of component i in shell side (atm)

P_{tT}	total pressure of component i in tube side (atm)
P_{ti}	partial pressure of component i in tube side (atm)
S_{ij}	stoichiometric coefficient for component i in the j^{th} reaction
k_1	Rate constant for reforming reaction (mol $gcat^{-1}$ s^{-1})
k_2	Rate constant for RWGS reaction (mol $atm^{-1}gcat^{-1}$ s^{-1})
ρ_b	the catalyst bed density on tube side in (kgm^{-3})
ΔH_{298}	the standard heat of reaction (kJ mol^{-1})
d	thickness of membrane (m)
i	total number of components involved
j	total number of reactions taking place in a reactor
J_i	membrane flux for i^{th} component,(mole sec^{-1} m^{-2})
K_1	equilibrium constant for methane reforming reaction
K_2	equilibrium constant for RWGS reaction
K_3	equilibrium constant for methane cracking reaction
K_4	equilibrium constant for boudard reaction
K_5	equilibrium constant for CO reduction reaction
K_6	equilibrium constant for CO_2 reduction reaction
M_i	molecular weight of component i, (kg $kmole^{-1}$)
r	pore radius of membrane,(m)
R	gas constant in (J/mole.K)
R_1	inner radius of the tube (m)
R_2	outer radius of the tube, (m)
R_3	inner radius of the shell, (m)
T	temperature, (K)
Z	length of the reactor, (m)
η_j	effectiveness factor

CHAPTER 1
INTRODUCTION

1.1 SYNGAS

In recent years greater attention has been paid towards the global warming, which has resulted due to increase in greenhouse gases emission in atmosphere. CO_2 and CH_4 are major greenhouse gas contributors (being 9-26% and 4-9% respectively). So measures are to be taken for proper utilization of these gases to limit their emission. Dry reforming of methane (DRM) is a potential method to reduce the emission of CO_2 and CH_4 to the atmosphere by their utilization to produce higher value added chemicals like syngas and satisfy raw material requirement for various synthetic process in industries.

Syngas is a gas mixture that contains varying amount of hydrogen(H_2) and carbon monoxide(CO). It is a versatile feedstock for methanol, Fischer-Tropsch process and DME production. Steam reforming is the traditional way for the production of syngas but it has a major drawback that it produces syngas with a H_2/CO ratio of 3:1 and this is higher than that needed for Fischer-Tropsch and methanol production process. Thus synthetic gas production by dry reforming route is an attractive option since it produces syngas with a H_2/CO ratio of 1:1 and at the same time this reaction has a very important environmental benefit since both CO_2 and CH_4 contribute to the greenhouse effect and converting these gases into a valuable feedstock significantly reduce the atmospheric emissions of these gases.

The dry reforming reaction is highly endothermic and thus it is high energy consuming process. Due to the absence of effective and stable catalyst there has not been instituting of any industrial technology for DRM. Various studies have and are being carried out in order to develop an active and stable catalyst for dry reforming of methane. Both noble(Rh, Pd, Pt, Ru) and non-noble catalysts mainly nickel based catalyst have been investigated for the production of syngas. But still carbon formation remains the leading cause for the deactivation of the catalyst. Thus, it is important to obtain the optimum conditions considering the carbon formation, so that the reaction can be carried out at the conditions where the catalyst remains active and the performance of the overall process is improved.

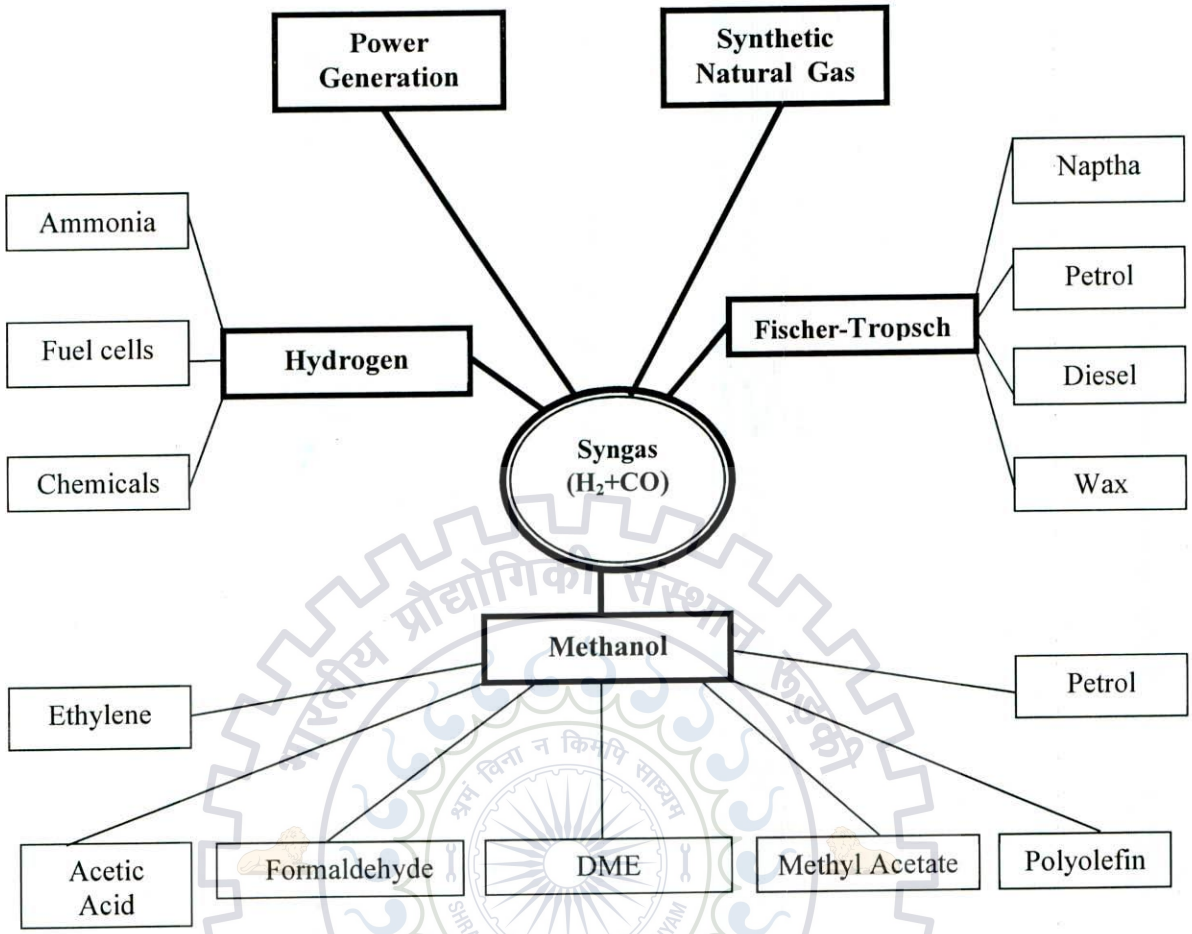

Fig 1.1: Different ways in which syngas can be used

1.1 METHOD OF PRODUCTION OF SYNGAS (H_2+CO)

Significant attention has been paid towards the efficient commercial production of syngas (mixture of H_2 and CO) because of the increasing demand of chemicals and synthetic fuels in today's world. There are four processes for the production of syngas, namely:

- Steam reforming,
- Partial oxidation,
- Auto thermal reforming and
- CO_2 reforming (dry reforming).

1.2.1 Steam Reforming

Steam methane reforming is a well-known and traditionally used commercial technology for converting methane into synthesis gas and is most widely used in the world at present. It produces Syngas with a H_2/CO ratio of approximately 3:1 to 5:1. It is generally carried out at a temperature of 1100-1200K and at a pressure ranging from 15-30 atm. In steam reforming process the reforming reaction is usually accompanied by water gas shift(WGS) reaction. The two reactions are given as:

$$CH_{4\,(g)} + H_2O_{(g)} \leftrightarrow CO_{(g)} + 3H_{2\,(g)} \quad \Delta H_{298K} = 206.0 \text{ kJ/mol} \quad \ldots\ldots\ldots\ldots\ldots\ldots\ldots\ldots (1.1)$$

$$CO_{(g)} + H_2O_{(g)} \leftrightarrow CO_{2\,(g)} + H_{2\,(g)} \quad \Delta H_{298K} = -41.2 \text{ kJ/mol} \quad \ldots\ldots\ldots\ldots\ldots\ldots\ldots\ldots (1.2)$$

Continuous research work is being done to improve the catalyst, heat transfer and operating conditions, but still the main disadvantages associated with the process are:

- High operating temperature and pressure,
- Coke formation on catalytic surface and,
- High endothermicity of the reaction.
- The syngas H_2/CO ratio of 3:1 to 5:1 is obtained which is higher than that needed for Fischer-Tropsch or methanol synthesis.
- Occurring of water gas shift reaction parallel to reforming reaction produces carbon dioxide which has a negative effect on environment as far as global warming is concerned.

So on the basis of above reasons the dry reforming of methane (DRM) is getting more attention as an alternative to steam reforming of methane (SRM) .

1.2.2 Partial Oxidation

In partial oxidation, the CH_4 is reacted with limited amount of O_2 (in the presence of catalyst) that is not enough to oxidize the CH_4 completely to CO_2 and H_2O.

$$CH_{4\,(g)} + (1/2)O_{2(g)} \leftrightarrow CO_{(g)} + 2H_{2(g)} \quad \Delta H_{298K} = -36.0 \text{ kJ/mol} \quad \ldots\ldots\ldots\ldots\ldots\ldots\ldots\ldots (1.3)$$

Partial oxidation of methane is exothermic in nature which results in low energy consumption and this is one of the most important advantage of this process over the conventional steam reforming. But as other processes partial oxidation of methane also has its limitations such as:

- the cost of pure oxygen supply for partial oxidation process,

- high temperature in the reactor (>1773K), which results in formation of hot spots on reactor material surface, and
- Possible occurrence of carbon deposition, by the CO reduction reaction, Boudouard reaction and CH_4 decomposition reaction.

The above limitations lead to high cost of reactor material and soot formation.

1.2.3 Auto-thermal Reforming (ATR)

Auto thermal reforming of methane is a combination of partial oxidation and steam reforming of methane. The process takes place at temperature of about 1400K and at a pressure of about 20 atm.The syngas produced has H_2/CO ratio of 2.0. The main reactions involved in auto thermal reforming of methane are:

$$CH_{4\,(g)} + (3/2)\,O_{2\,(g)} \leftrightarrow CO_{(g)} + 2H_2O_{(g)} \qquad \Delta H_{298K} = -520.0 \text{ kJ/mol} \quad \ldots\ldots (1.4)$$

$$H_2O_{(g)} + CH_{4\,(g)} \leftrightarrow CO_{(g)} + 3H_{2\,(g)} \qquad \Delta H_{298K} = +206.0 \text{ kJ/mol} \quad \ldots\ldots (1.5)$$

$$CO_{(g)} + H_2O_{(g)} \leftrightarrow CO_{2\,(g)} + H_{2\,(g)} \qquad \Delta H_{298K} = -41.20 \text{ kJ/mol} \quad \ldots\ldots (1.6)$$

Auto thermal reforming of methane is carried out in two separate reaction zones—

- First zone: combustion of a part of methane is carried out in a flame or catalytic burner which produces a hot product stream having a temperature of about 1400 °C.
- Second zone: conversion of methane(unconverted) by steam reforming process to syngas by the products obtained from the previous combustion zone that are H_2O and CO_2.

Using such a process for syngas production provides a major advantage that is no external energy is used as the energy from the exothermic partial oxidation reaction is provided by endothermic steam reforming reaction. This results in a lower temperature of the auto-thermal process. As the temperature is low there is production of CO_2 and H_2 as at low temperature water gas shift reaction is favoured. The main disadvantages associated with the process are:

- production of large amount of carbon dioxide as one of the products,
- the catalyst fouling (deactivation) resulting from the high-temperature of about 1400 °C
- requirement of pure oxygen, and

- thermal shocks received by the catalyst, especially during the periods of process start-up and shutdown.

1.2.4 Dry Reforming (CO_2 Reforming)

The dry reforming of methane(DRM) to synthesis gas is an attractive route for production of chemicals as the syngas produced has H_2/CO ratio of 1:1 which is desirable for many industrial synthesis processes mainly Fischer-Tropsch synthesis.

Also dry reforming of methane constitutes a promising option for the conversion of natural gas into syngas mainly due to the environmental benefits that it offers. Also this reaction has a very important environmental benefit since both CO_2 and CH_4 contribute to the greenhouse effect and converting these gases into a valuable feedstock significantly reduce the atmospheric emissions of these gases. The main reactions involved are the reforming reaction, RWGS reaction and four carbon formation reactions.

Methane reforming reaction:

$$CH_{4\,(g)} + CO_{2\,(g)} \leftrightarrow 2CO_{(g)} + 2H_{2\,(g)} \qquad \Delta H_{298K} = 247.0 \text{ kJ/mol} \quad \text{.....(1.7)}$$

Reverse water gas shift reaction:

$$H_{2\,(g)} + CO_{2\,(g)} \leftrightarrow CO_{(g)} + H_2O_{(g)} \qquad \Delta H_{298K} = +41.0 \text{ kJ/mol} \quad \text{.....(1.8)}$$

To obtain lower H_2/CO ratio (=1) the carbon dioxide reforming of methane is carried out with excess CO_2 to promote reverse water gas shift reaction(RWGS). The dry reforming reaction is slightly more endothermic then steam reforming so, it is favoured at low pressure of 1atm and a temperature of about 800-1200 K. It has been evaluated that the CO_2 reforming provides about 20% lower operating cost than any other reforming processes.

Thus methane reforming with CO_2 is an efficient and cost effective way of utilizing the two greenhouse gases (CO_2 and CH_4) for the production of syngas. However the deactivation of catalyst caused by carbon formation and its deposition on the surface of catalyst is among one of the major and serious problem of this reaction. Thermodynamically, the most probable reactions leading to carbon formation during CO_2 reforming are as follows:

Boudouard reaction:

$$2CO \leftrightarrow CO_2 + C \qquad \Delta H_{298K} = -172.0 \text{ kJ/mol} \quad \text{.....(1.9)}$$

Methane cracking reaction:

$CH_4 \leftrightarrow 2H_2 + C$ $\Delta H_{298K} = +75.0$ kJ/mol .....,.....(1.10)

CO reduction reaction:

$CO + H_2 \leftrightarrow H_2O + C$ $\Delta H_{298K} = -131.0$ kJ/mol .....(1.11)

CO_2 reduction reaction:

$CO_2 + 2H_2 \leftrightarrow 2H_2O + C$ $\Delta H_{298K} = -90.0$ kJ/mol .....(1.12)

As a result of these carbon formation reactions, different amounts and types(structure) of carbonaceous species form, depending on the several factors, which include type of catalyst support, chemical properties, size of metallic particles, operating temperature and pressure, CH_4/CO_2 feed ratio, and metal morphology.

1.2 OBJECTIVES

1. To conduct thermodynamic analysis of the dry reforming of methane.
2. To compute production of H_2, CO & carbon formation.
3. To analyze the effect of molar feed ratio of CH_4 & CO_2 in feed on H_2/CO ratio, H_2 yield, H_2 selectivity, CH_4 conversion and carbon formation.
4. To study the effect of H_2 addition in feed on H_2/CO ratio, H_2 yield, H_2 selectivity, CH_4 conversion and carbon formation.
5. To study the effect of change in temperature on above objectives.
6. To develop a model for dry reforming of methane.
7. To solve the model equations for different reactor configurations.
8. To validate the model with experimental data on reactors available in literature.

CHAPTER 2

LITERATURE REVIEW

Various studies have been done for the development of active and coke-resistant catalysts for the dry reforming of methane(DRM) reaction. Commonly used supported metal catalysts for methane reforming reaction are from groups VIII (ruthenium), IX (cobalt, rhodium, and iridium), and X (nickel, palladium and platinum). Noble metals catalysts are reported to be more active and less sensitive towards coking, but they have the limitation of being costly and less availability. Among the commonly used catalysts, Ni-based catalysts are considered as an economical choice for the dry reforming of methane industrially.

The development of cheap and economical catalysts for methane reforming reactions, which are resistant to coke formation and exhibit high activity are important, as far as industrial applications are considered. So to improve the coke resistance of Ni-based catalysts effect of various supports and promoters have been investigated. Also, combination of two or three metals as active sites have been carried out for the improvement of catalytic activity and limit coke formation. Different type of catalyst preparation methods have also been investigated to minimize costs and extend the lifespan of catalysts.

Supports are important part of a catalyst. The use of support makes the metal catalyst affordable and acts as a vehicle for the active sites. It increases the surface area of the active sites by providing a large area, and makes catalyst suitable for use in the reactor. Various catalysts supports such as silica, alumina, zirconia, and others mesoporous materials have been considered for dry reforming of methane. Usually the support is not active catalytically, but in some cases the support along with the metal active sites participates in the total reaction in a significant way.

2.1 EXPERIMENTAL AND MODELING WORK

Sokolov et al., 2012 prepared different Nickel catalysts with various supports. The catalysts were tested at low temperature of 400°C for dry reforming of methane(DRM). For Ni/La_2O_3-ZrO_2 catalyst almost equilibrium values for yields of hydrogen and carbon monoxide were obtained. Also, it exhibited the highest stability. This catalytic activity and stability were studied on the basis of catalyst support morphology. It was found that if all the supports had same tetragonal crystalline phase, the performance of carbon dioxide reforming of methane

depended on the morphology of La_2O_3-ZrO_2 support. The results obtained showed that no change in activity was obtained for Nickel supported on the mesoporous La_2O_3-ZrO_2 for over 180 h on-stream. But approximately 20% of the catalytic activity for Nickel supported on the non-structural and macro porous La_2O_3-ZrO_2 was lost over 100 h on stream.

Liu, et al., 2012 , used different pre-treatment atmospheres for studying the dry reforming of methane over Ni/ZrO_2-SiO_2 catalyst. Different characterization techniques were used and the results obtained it showed that the type of gas used in the pre-treatment has an important effect on the catalyst performance. The different gases used for pre-treatment were helium, hydrogen and carbon monoxide. The results obtained by pre-treating the catalyst with these gases were:

- *helium-pre-treated catalyst*
  - Improved the generation of well distributed active metal sites, showing improved performance.
- *H_2 pre-treatment catalyst*
  - considerably degraded catalytic activity of metal sites.
- *CO pre-treatment catalyst*
  - carbon encapsulated metal species formation took place resulting in severe catalytic deactivation.

On the basis of various results obtained it was concluded that He pre-treated catalyst is the most suitable catalyst for this application.

Gamba et al., 2011, modified the mineral clay support for Ni–Pr catalyst with Aluminium, microwaves and polyvinyl alcohol [PVA]. The catalyst was then used in the dry reforming of methane reaction. The experimental conditions used were:
Feed ratio of 50/50 CH_4/CO_2 mixture, flux of 80 mL min^{-1}, WHSV = 96 $lg^{-1}h^{-1}$(without dilution gas) and no previous reduction and time period of 300 min. The effect of calcination temperatures (500 °C and 800 °C) and the addition of Pr(0, 1, 3 and 5%) in different percentages on the catalyst was studied. The results obtained showed that the calcination temperature had a considerable effect on the coke formation on the catalytic surface as influenced the NiO species formation which in turn had an effect on the activity of the catalyst. Also the activity of the catalyst increases on the addition of Pr resulting in increased conversion of methane and carbon dioxide. No coke formation was obtained fro catalyst calcinated at 800 °C.

Kang et al., 2011 prepared Ni/Al_2O_3 and $Ni/MgO–Al_2O_3$ catalysts with core/shell structures for the use in CO_2 reforming of methane. Both the catalysts had 10% Nickel loading. The catalyst had been used for steam reforming of methane, giving a CH4 conversion of 97% at 750°C and for the partial oxidation of methane, obtaining a CH4 conversion of 96% at 800°C. When used for CO_2 reforming of methane it showed great thermal stability for 150 h of operation. The conversions obtained for the two catalysts at 800°C and with a molar ratio of $CH_4/CO_2 = 1$ were:

Catalyst	CH_4 conversion %	CO_2 conversion %
Ni/Al_2O_3	92	95
$Ni/MgO–Al_2O_3$	92.5	91.8

The values were near equilibrium values.

Al-Fatesh et al., 2011, investigated the dry reforming of methane on $Ni/\alpha\text{-}Al_2O_3$ and Ni/TiO_2-P25 supported catalyst. In addition the effect of adding Zr and Ce promoters was also studied. Experimental investigations over the catalysts were carried out at flow rate of 33 ml/min, pressure of 1 atm and temperature ranging from 500°C and 800°C. The effect of various operating conditions such as space velocity, feed ratio, and oxygen addition on catalyst stability, activity and H_2/CO ratio were studied. The result obtained on the basis of various characterization techniques showed that higher promotion and stability were obtained when Zr was added, also carbon formation was very low at a temperature of 800°C. In case of 1%Ni+0.15%Zr catalyst over 80% $\alpha\text{-}Al_2O_3$+20% TiO_2 support, for a feed ratio CO_2/CH_4 of 1.3 at a temperature of 800°C methane and carbon dioxide conversions were found to be 97% and 89.5% respectively.

Aksoylu et al.,2011 synthesized and then tested Pt-Ni bimetallic catalysts supported on $\delta\text{-}Al_2O_3$ for use in the syngas production by dry reforming of methane(DRM). The aim of the experiment was to optimize this catalyst so as to obtain higher stability and activity. The results showed that:

- the performance of Pt-Ni bimetallic catalyst greatly depends on the Ni/Pt loading ratio and the metal loadings.
- The catalytic activity was high for 0.3% Pt-10%Ni/Al_2O_3 catalyst, it had the lowest Ni/Pt ratio.

The reason for such behaviour was revealed by combined catalyst performance and characterization tests according to which when Ni/Pt loading ratio is low, nickel oxide easy reduction takes place leading to small(Nano-sized) Ni particles, thus improved dispersion resulting from intimate interaction between Pt and Ni sites(in the closed vicinity).

Monroy et al., 2010, synthesized and studied 15% Ni/MgO-ZrO catalyst for dry reforming of methane. The catalyst is believed to have excellent stability and activity because of high basicity of MgO and at the same time the presence of mobile oxygen species provided by ZrO_2. Impregnation method of synthesis was used for catalyst preparation resulting in MgO/ZrO_2 mole ratio of 1. The steps followed during experimentation were:

- Catalyst was placed inside a quartz reactor (U-tube) and inserted into a tube furnace.
- Reaction was carried at a temperature of 850 ^{o}C
- At a total flow rate of 100ml/min the reactants methane and carbon dioxide along with the inert carrier gas helium were injected into the reactor.
- For the determination of exit gas(unreacted reactants, products & inert) composition an on-line gas chromatograph was used.

On the basis of results obtained it was concluded that surface properties of Ni/MgO catalyst changed by the addition of ZrO_2. The results obtained were that:

- 15% Ni/MgO-ZrO_2 had a lower surface area than 15% Ni/MgO.
- 15% Ni/MgO-ZrO_2 had lower number of basic sites as compared to that in 15% Ni/MgO.
- 15% Ni/MgO-ZrO_2 gave higher CH_4 conversion and low carbon deposition.
- 15% Ni/MgO-ZrO_2 had a crystalline structure that was almost same to that of Ni/ZrO_2, which may results in lower catalyst activity in spite of the high resistance for carbon deposition.

On the basis of results obtained it was concluded that catalytic performance can be improved by using proper catalytic preparation technique. It was also recommended that other synthesizing techniques like co-impregnation and sol-gel methods should be studied so as to improve the catalytic technology for dry reforming of methane.

Djaidja et al., 2009, studied catalysts prepared by co-precipitation method and compared it with that prepared by the conventional impregnation method. In both catalysts it was observed that catalytic activity increased when both catalysts were reduced in H_2 atmosphere

but as the pre-treatment temperature increased, decreasing reducibility was observed in both the catalysts. Using different analysis techniques, it was found that deposition of carbon on both the catalysts contained surface carbon, Ni carbide, carbon nanotubes and CHx species. The results obtained showed that better reducibility (with pre-treatment) and better Nickel particle distribution was obtained for both the catalysts thus, making them a good choice for carbon dioxide reforming of methane to produce syngas with good yields and with less carbon deposition.

Junke XU et al., 2009, prepared $Ni/La_2O_3/\gamma\text{-}Al_2O_3$ and $Ni/La_2O_3/\alpha\text{-}Al_2O_3$ catalysts using two different preparation techniques that are evaporation methods and incipient wetness impregnation. Different characterization techniques for characterizing catalysts(fresh & used) and coke deposition were used. The results obtained showed that there were carbon deposited on catalytic surface existed as three forms, namely

- amorphous (polymeric),
- filamentous and
- graphitic carbon.

The type and amount of carbon deposition on the catalysts depended on two factors, firstly the size of Ni particles and secondly on the texture of the support. On the basis of results obtained they concluded that deposition and formation of filamentous carbons was in case when Ni particles size was less than 15 nm. It also decreased the carbon deposition and formation of active carbon species, thus giving better and higher stability as well as activity to the catalyst.

Pawelec et al., 2007, investigated the effect of addition Nickel in different percentages ranging from 1-12% on the catalytic behaviour of bimetallic Pt-Ni catalysts supported on ZSM-5 for dry reforming of CH_4 to produce syngas. The effect of addition of 0.5% Pt was also studied and it was observed that it increased NiO reduction as smallNiO particle formation takes place. Also, the increase in the Nickel dispersion increased/improved the stability and activity of the catalyst as the contact between Ni and Pd improved and was best at 6wt% loading.

Nowosielska et al., 2005, investigated the stability and activity of monometallic Rh, Ni and bimetallic Ni–Rh catalysts supported on silica, for the dry reforming of methane to syngas. On the basis of results obtained the main conclusions drawn out were:

- the SiO_2 supported Rh, Ni and bimetallic Ni–Rh catalysts are comparably good catalysts for DRM.
- Catalysts rich in Rhodium are resistant to carbon formation and deactivation.
- Formation of Ni–Rh alloy takes place in the case of Ni–Rh /SiO_2 supported catalysts unless high temperature calcination(in oxygen stream) is carried out.
- Ni-rich surface alloy are formed by segregation of metals.

Chang et al., investigated the performance in terms of activity of two zeolite supported nickel based catalysts. The two catalysts differed in the processes of their synthesis. One was prepared by incipient wetness method and the other by solid-state reaction. The results showed that the catalyst synthesized by using solid-state reaction technique was more active than the one prepared by incipient wetness method. No deactivation(no or very less coke formation) was observed for over 140 h of operation. Also, at a temperature of 1073K reactants conversion of >90% and syngas with H_2/CO ratio of 1 was obtained. The reason proposed for such different behaviour of the catalysts was that in solid-state reaction there was melting effect of metallic precursor mixtures.

2.2 THERMODYNAMIC ANALYSIS (gibbs free energy minimization method)

Soria et al., 2011, carried out the thermodynamic equilibrium calculations for dry reforming of methane and investigated the effect of addition of steam in small amounts with the feed. Gibbs free minimization approach was used for the equilibrium composition calculation of the components. The thermodynamic results were compared with that obtained from experiment which was conducted to investigate the effect of co-addition of steam over a Ru/ZrO_2-La_2O_3 catalyst for the carbon dioxide reforming of methane. The experiment was carried out in a fixed bed reactor at a max. temperature of 550 °C. A good agreement between the experimental results and the thermodynamic predictions was obtained. The results indicated the the addition of steam:

- Increase in the stability of the Ru/ZrO_2-La_2O_3 catalyst
- Increased methane conversion
- Increased hydrogen yield

- Decreased carbon dioxide conversion
- Decreased carbon monoxide yield

On the basis of results obtained it was concluded that at any given temperature, the desirable syngas ratio(H_2/CO) can be obtained by changing the amount or percentage of steam co-added to the feed of DRM.

Demidov et al., 2011, investigated the combined steam and carbon dioxide reforming of methane by applying Gibbs free energy minimization approach to calculate the thermodynamic equilibrium composition of the components. The influence of various operating parameters likes temperature, pressure, H_2O/CH_4 and CO_2/CH_4 mole ratios on the methane conversion, syngas ratio and carbon deposition was also investigated. The optimum $CH_4/CO_2/H_2O$ ratio in the feed was obtained keeping in view:

- High conversions of methane and carbon dioxide are obtained,
- no coke formation takes place and
- the syngas H_2/CO ratio remains in the range of 2.1-2.2.

Instead of stoichiometric feed composition, when optimized $CH_4/CO_2/H_2O$ molar ratios were used it was possible to decrease the upper temperature limit of carbon deposition by 150 ^{0}C and reduce the content of methane in the product syngas to half. The results obtained indicated that if the total content of admixtures in synthetic gas is to be maintained below 13%, then using the optimized $CH_4/CO_2/H_2O$ molar ratios the operating conditions should be:

- at a pressure of 5 atm, the combined steam and carbon dioxide reforming of methane process can be conducted at 800 ^{0}C.
- at a pressure of 20 atm, the processes should be conducted at a temperature of 900 ^{0}C

M. Khoshtinat Nikoo et al., 2011, Performed a thermodynamic equilibrium analysis on the multi-reaction system for carbon dioxide reforming of methane in view of carbon formation with Aspen plus based on direct minimization of Gibbs free energy method. The effects of CO_2/CH_4 ratio (0.5–3), reaction temperature (573–1473 K) and pressure (1–25 atm) on equilibrium conversions, product compositions and solid carbon were studied. Numerical analysis revealed that the optimal working conditions for syngas production in Fischer–Tropsch synthesis were at temperatures higher than 1173 K for CO_2/CH_4 ratio being 1 at which about 4 mol of syngas (H_2/CO=1) could be produced from 2 mol of reactants with negligible amount of carbon formation. Although temperatures above 973 K had suppressed

the carbon formation, the moles of water formed increased especially at higher CO_2/CH_4 ratios. This increment was attributed to RWGS reaction attested by the enhanced number of CO moles, declined H_2 moles and gradual increment of CO_2 conversion. The simulated reactant conversions and product distribution were compared with experimental results in the literatures to study the differences between the real behaviour and thermodynamic equilibrium profile of CO_2 reforming of methane. The potential of producing decent yields of ethylene, ethane, methanol and dimethyl ether seemed to depend on active and selective catalysts. Higher pressures suppressed the effect of temperature on reactant conversion, augmented carbon deposition and decreased CO and H_2 production due to methane decomposition and CO disproportionation reactions. Analysis of oxidative CO_2 reforming of methane with equal amount of CH_4 and CO_2 revealed reactant conversions and syngas yields above 90% corresponded to the optimal operating temperature and feed ratio of 1073 K and $CO_2:CH_4:O_2$=1:1:0.1, respectively. The H_2/CO ratio was maintained at unity while water formation was minimized and solid carbon eliminated.

Yanbing et al., 2007, used the free energy minimization approach to investigate the influence of operating parameters that are CH_4/CO_2 ratio, temperature and pressure on CH_4 conversion, CO_2 conversion and products distribution in carbon dioxide reforming of methane. The results obtained were:

- Methane conversion:
  - increases with increase in temperature , decreases with increase in pressure and decreases with increase in CH_4/CO_2 ratio increases
- The syngas H_2/CO ratio increases with increase in CH_4/CO_2 ratio in the feed.
- On combining DRM with oxidation (addition of O_2 in the feed), an energy balance in the process was obtained.

On the basis of the results obtained it has been concluded that syngas H_2/CO ratio can be adjusted without RWGS reaction for Fisher-Tropsch process.

Table 2.1
Different types of catalysts used in DRM

Author	Catalyst	Support	Promoter	Preparation Method	Temp/P/molar ratio	Stability	H_2/CO	Conv CH_4 %	Conv CO_2 %	Space Velocity	Carbon Deposition
Benrabaa et al. (2013)	$NiFe_2O_4$ (spinel)	-	reduction by H_2	co-precipitation	800C/1/2	n.m.	0.09	7	20	54000 $mLh^{-1}gcat^{-1}$	n.m.
	$NiFe_2O_4$ (spinel)	-	not used	hydrothermal synthesis	800C/1/2	n.m.	0.1	13.5	34	54000 $mLh^{-1}gcat^{-1}$	n.m.
	$NiFe_2O_4$ (spinel)	-	not used	sol gel	800C/1/2	stable	1.2	80	95	54000 $mLh^{-1}gcat^{-1}$	n.m.
Odedairo et al., (2013)	Ni	CeO_2	not used	wet impregnation + thermally calcined	700C/1/1	n.m.	0.625	43	81	38400 $mLh^{-1}gcat^{-1}$	n.m.
	Ni	CeO_2	not used	wet impregnation + plasma treated	700C/1/1	n.m.	0.64	47	82	38400 $mLh^{-1}gcat^{-1}$	n.m.
Alonso, et al. (2013)	Ni (1wt %)	alumina	not used	excess solution impregnation	1073K/-/1	stable	n.m.	74	n.m.	22,000 h^{-1}	<0.01
	Co(2.5%)	alumina	not used	excess solution impregnation	1073K/-/1	stable	n.m.	61	n.m.	22,000 h^{-1}	<0.01
Sokolov et al. (2012)	Ni (5 wt.%)	La_2O_3-ZrO_2	not used	urea hydrolysis method	400C/1/1	180h	-0.553	n.m.	n.m.	7200 mL h^{-1} g_{cat}^{-1}	n.m.
Kang et al. (2011)	Ni (10wt %)	Al_2O_3,	not used	multi-bubble sonoluminescence	800C/1/1	150 h	-0.93	92	95	-	3.08 mg/mg Catalyst
	Ni (10wt %)	MgO–Al2O3	not used	multi-bubble sonoluminescence	800C/1/1	150h	-0.94	92.5	91.8	-	n.m.
Alonso et al. (2009)	Ni(7.7%)	alumina	not used	excess volume impregnation	973K/-/1	n.m.	n.m.	60	66	22,000 h^{-1}	41 mg/g catalyst
	Co(7.6%)	alumina	not used	excess volume impregnation	973K/-/1	n.m.	n.m.	75	83	22,000 h^{-1}	290 mg/g catalyst

	Ni-Co (8.3-.8)	alumina	not used	excess volume impregnation	973K/-/1	n.m.	n.m.	60	67	22,000 h^{-1}	20 mg/g catalyst
	Ni-Co (4.3-3.5)	alumina	not used	excess volume impregnation	973K/-/1	n.m.	n.m.	66	71	22,000 h^{-1}	49 mg/g catalyst
	Ni-Co (.8-7.2)	alumina	not used	excess volume impregnation	973K/-/1	n.m.	n.m.	72	80	22,000 h^{-1}	268 mg/g catalyst
Haag et al. (2007)	Ni–Co	Al_2O_3	not used	co-precipitation	550C/-/1	nd	0.93	39.3	52.7	3000h^{-1}	n.m.
	Ni	Al_2O_3	not used	co-precipitation	550C/-/1	nd	1.06	50	58	3000h^{-1}	n.m.
Gallego et al. (2006)	$LaNiO_3$	perovskites	H_2 tretd	self-combustion	700C/1/1	n.m.	0.82	65	81	3×10^5 mL h^{-1} g^{-1}	2.8 (wt%)
	La_2NiO_4	perovskites	H_2 tretd	self-combustion	700C/1/1	n.m.	0.84	80	90	3×10^5 mL h^{-1} g^{-1}	2.7(wt%)
	1% Ni	La_2O_3	H_2 tretd	wet impregnation	700C/1/1	n.m.	0.47	32	48	3×10^5 mL h^{-1} g^{-1}	2.6(wt%)
	5% Ni	La_2O_3	H_2 tretd	wet impregnation	700C/1/1	n.m.	0.66	59	73	3×10^5 mL h^{-1} g^{-1}	3.2(wt%)
	17% Ni	La_2O_3	H_2 tretd	wet impregnation	700C/1/1	n.m.	0.84	62	75	3×10^5 mL h^{-1} g^{-1}	12(wt%)
	$LaNiO_3$	perovskites	not used	self-combustion	700C/1/1	n.m.	0.68	60	75	3×10^5 mL h^{-1} g^{-1}	2.7(wt%)
	La_2NiO_4	perovskites	not used	self-combustion	700C/1/1	n.m.	1.03	80	90	3×10^5 mL h^{-1} g^{-1}	70(wt%)
Munera et al. (2003)	0.6% Rh	La_2O_3	not used	wet impregnation	550C/1/1	stable	n.m.	26	41	2000 $mLh^{-1}gcat^{-1}$	n.m.
	0.93% Pt	La_2O_3	not used	wet impregnation	550C/1/1	n.m.	n.m.	26.3	38.2	2000 $mLh^{-1}gcat^{-1}$	n.m.

Liu et al. (2003)	Ni	θ-Al_2O_3	La_2O_3	wet impregnation	1073K/1/1	n.m.	0.924	84	85.2	-	n.m.
	6.80% Ni	41% Al_2O_3	4.3	wet impregnation	1073K/1/1	n.m.	0.961	96	94.7	-	n.m.
	7% Ni	37.2% Al_2O_3	10.5	wet impregnation	1073K/1/1	n.m.	0.992	97	96.6	-	n.m.
	7.30% Ni	33.9% Al_2O_3	16.7	wet impregnation	1073K/1/1	n.m.	0.954	87	88.8	36000 $mLh^{-1}gcat^{-1}$	n.m.
Nagaoka et al. (2001)	Ru	SiO_2,	not used	wet-impregnation	1023K/2MPa/1		n.m.	20	23	.0093gh^{-1}	16.4(wt%)
	Ru	Al_2O_3	not used	wet-impregnation	1023K/2MPa/1		n.m.	35	39	0093gh^{-1}	19.5(wt%)
	Ru	MgO	not used	wet-impregnation	1023K/2MPa/1		n.m.	39	44	0093gh^{-1}	1.2(wt%)
	Ru	TiO_2	not used	wet-impregnation	1023K/2MPa/1	stable	n.m.	28	30	0093gh^{-1}	no deposition
Prabhu et al. (1999)	Ni	MgO	not used	co-precipitating	650/1/1 (1.125Ar)	n.m.		62.5	73	-	n.m.
	Ni	La_2O_3	not used	co-precipitating	650/1/1 (1.125Ar)	n.m.		62.5	73	-	n.m.
Wang and Lu (1999)	Ni	Y-Al_2O_3,	Not used	wet impregnation	700C/1/1	1-5h rapid	n.m.	79	83	18000 $mlh^{-1}gcat^{-1}$	14.3% (140h)
Wang and Lu (1998)	Ni	Y- Al_2O_3	$Ni(NO_3)_2$	wet-impregnation	700C/1/1	stable		68	71	18000 $cm^3h^{-1}gcat^{-1}$	n.m.
	Ni	Y- Al_2O_3	nickel chloride,	n.m.	700C/1/1	n.m.		71	72	18000 $cm^3h^{-1}gcat^{-1}$	n.m.
	Ni	Y- Al_2O_3	nickel acetyl acetone	n.m.	700C/1/1	n.m.		79	82	18000$cm^3h^{-1}gcat^{-1}$	n.m.

Galuszka et al. (1998)	Pd	Al_2O_3	not used	n.m.	550C/-/1			17.2	24.6	5714mlmin^{-1}gcat^{-1}	n.m.
Wang and Au (1997)	Rh(<.5%)	SiO_2,	not used	wet impregnation	750C/1/1	n.m.	n.m.	61	75	-	n.m.
	Rh(>=1%)	SiO_2,	not used	wet impregnation	750C/1/1	n.m.	n.m.	66	72	-	n.m.
	Rh(8%)	SiO_2,	not used	wet impregnation	750C/1/1	n.m.	n.m.	61	66	-	n.m.
	Rh(<.5%)	SiO_2,	not used	wet impregnation	800C/1/1	n.m.	n.m.	93	89	-	n.m.
	Rh(>=1%)	SiO_2,	not used	wet impregnation	800C/1/1	n.m.	n.m.	95	83	-	n.m.
	Rh(8%)	SiO_2,	not used	wet impregnation	800C/1/1	n.m.	n.m.	96	75	-	n.m.

CHAPTER 3

MATHEMATICAL MODELLING

3.1 MODEL DEVELOPMENT

Mathematical models serve as an invaluable tool for better understanding of the chemical processes occurring in a chemical reactor. Model is a mathematical representation of the actual process. Its basis includes the fundamental law of mass, energy and momentum. Also the constitutive relations associated with the reaction system are to be considered.

In the present study two major reactions, namely dry reforming reaction and reverse water gas shift reaction has been considered for DRM in membrane and fixed bed reactors. Steady state, 1D, isothermal model for DRM carried out in membrane reactor and fixed bed reactor has been considered. For the development of model various parameters and properties associated with the reaction system have been considered. These model equations are to be solved in conjugation with the equations for constitutive properties. The relationship for constitutive properties includes expressions for:

- Rates of reactions,
- Kinetic parameters,
- Permeation of gaseous components through membranes,
- Characteristics of membranes and
- Catalyst used.

For the commercial application of the catalyst, its activity and stability are most important. Coke or carbon formation on the surface of the catalyst is the main reason for the catalyst deactivation. So it is important to know the range of operating conditions for which there will be no or very less carbon formation on catalyst surface. So the possibility of coke formation has been explored by carrying out the thermodynamic analysis of the coke forming reactions.

Fig 3.1 and fig 3.2 represents the schematic diagrams describing the processes in tubular and membrane reactors. Fixed bed reactor has simple tube like structure packed with catalyst whereas the membrane reactor is equipped with tubular membrane and has a shell

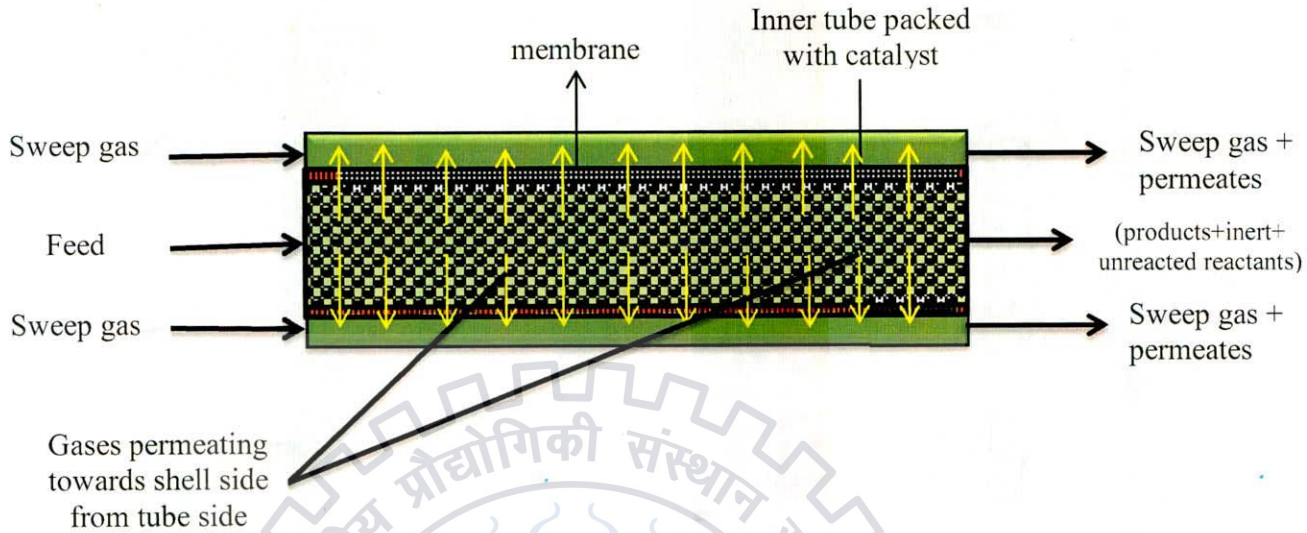

Fig 3.1: Schematic Representation of Membrane Reactor.

Fig 3.2: Schematic Representation of Fixed Bed Reactor.

and tube structure. The tube made up of supported composite membrane is packed with catalyst. The reactions take place at the tube side so it is known as reaction zone whereas the gases permeate through the membrane (which is inert in nature with respect to chemical reactions) to the shell side zone known as permeation zone. The shell is a non-permeable outer tube through which only heat may get transferred.

For the development of 1-D mathematical model for membrane reactor, a small elemental volume section is considered. For that small elemental length segment of size dz (keeping cross sectional area of reactor constant) is considered. Around the control volume material balance for each component has been considered for the formulation of model equations. Kumar et al. (2006) has provided comprehensive model for membrane reactor and that could be directly used to obtain these model equations. For the development of model following assumptions have been used:

3.1.1 Assumptions

The model equations are developed on the basis of following assumptions.

- The tube and the shell side of the reactor operate under steady state conditions.
- The reaction is carried out isothermally in the reactions. This can be justified by:
  - Supplying sufficient heat from the wall of the fixed bed reactor to maintain an approximately constant reaction temperature (in endothermic reforming reactions.)
  - In the membrane reactor, the use of a sweep gas in the shell can supply sufficient heat required to carry out the reaction in the reactor.
- The transport mechanism is considered to be of PFR type in the axial direction of both reaction and permeation zone.
- Ideal gas flow is assumed to be applicable inside the reactor as temperature inside the reactor is high and pressure is low.
- The membrane support does not offer resistance to gas permeation, therefore mass transfer resistance in the support layer on both surfaces of the membrane are neglected.
- Resistance offered by the gas film on the both sides of the membrane is neglected.

- Isobaric condition.
- The radial dispersion is also assumed to be negligible with the current reactor geometry.

3.1.2 Reactions Considered

For the development of model equation all the dry reforming reactions are considered that are presented in section 1.2.4. The reactions considered include methane reforming reaction, RWGS reaction, and the four carbon formation reactions i.e., equations (1.7) to (1.12). by considering these six reactions the total number of components for which mass balance equations are to be applied are seven (CH_4, CO_2, CO, H_2, N_2, H_2O & C).

3.2 MEMBRANE REACTOR MODEL

In this section the mass transfer equation for transport through tube, shell and membrane have been presented. In the mass transfer equations the +ve sign with r_i is used for those components which are produced while a –ve sign with r_i is used for those components which are being consumed. The mass transfer equation for a component i on tube and the shell side are given in the following subsections.

3.2.1 Reaction Zone (Tube Side)

The feed consisting of CH_4, CO_2 and N_2 is introduced into the tube side of the reactor. The feed flows through the packed bed where the reaction takes place. Thus after reaction taking place there are a total of seven components that include reactants, products and the inert. A control volume of length Δz has been considered and the mass balance has been applied over that control volume. The general mass balance equation around the control volume for any component *i* is given by:

$$\frac{dF_{ti}}{dz} - \pi R_1^2 \ \rho_b \sum_{j=1}^{n_1} \eta_j \left(\pm S_{ij} r_j\right) \pm 2\pi R_1 J_i = 0 \qquad i = 1 \ to \ n_2 \tag{3.1}$$

भारतीय प्रौद्योगिकी संस्थान रुड़की
श्रमं विना न किमपि साध्यम्
SHRAMAM VINA NA KIMAPI SADHYAM
INDIAN INSTITUTE OF TECHNOLOGY ROORKEE

The above mass transfer equations for the seven components are written in simplified form as follow:

- $\frac{dF_{tCH4}}{dz} - \pi R_1^2 \rho_b(-r_1 - r_3) + 2\pi R_1 J_{CH4} = 0$ (3.2)
- $\frac{dF_{tCO2}}{dz} - \pi R_1^2 \rho_b(-r_1 - r_2 + 0.5r_4 - r_6) + 2\pi R_1 J_{CO2} = 0$ (3.3)
- $\frac{dF_{tCO}}{dz} + \pi R_1^2 \rho_b(-2r_1 - r_2 + r_4 + r_5) + 2\pi R_1 J_{CO} = 0$ (3.4)
- $\frac{dF_{tH2}}{dz} + \pi R_1^2 \rho_b(-2r_1 + r_2 - 2r_3 + r_5 + 2r_6) + 2\pi R_1 J_{H2} = 0$ (3.5)
- $\frac{dF_{tN2}}{dz} + 2\pi R_1 J_{N2} = 0$ (3.6)
- $\frac{dF_{tH2O}}{dz} + \pi R_1^2 \rho_b(-r_2 - 2r_6 - r_5) + 2\pi R_1 J_{CO} = 0$ (3.7)
- $\frac{dF_{tC}}{dz} - \pi R_1^2 \rho_b(r_3 + 0.5r_4 + r_5 + r_6) = 0$ (3.8)

The +ve sign with J_i represents that the component is permeating from tube side (reaction side) to shell side (permeate side) while -ve sign with J_i represents that the component is permeating from shell side to tube side.

The mass balance equations for the fixed bed reactor are similar as that for tube side equations of membrane (Eqs. ((3.2)-(3.8)) except that the permeation term is zero for each component as there is no permeation zone in FBR.

3.2.2 Permeation Zone (Shell Side)

The N_2 is used as a sweep gas on the shell/permeate side of the reactor. In some cases the sweep gas used is reactive and thus reactions also occur on the shell/permeate side of the reactor. In our case the sweep gas nitrogen is inert so no reaction takes place on the shell side.


भारतीय प्रौद्योगिकी संस्थान रुड़की
श्रमं विना न किमपि साध्यम्
SHRAMAM VINA NA KIMAPI SADHYAM
INDIAN INSTITUTE OF TECHNOLOGY ROORKEE

Thus the reaction term in the mass balance equation is zero for all components that permeate towards the shell side including the sweep gas Nitrogen. The general mass balance equation around the control volume for any component i on the permeate side is given by:

$$\frac{dF_{si}}{dz} - 2\pi R_2 J_i = 0 \tag{3.9}$$

So the mass balance equations for all the components on the shell side are given as:

- $\frac{dF_{sCH4}}{dz} - 2\pi R_2 J_{CH4} = 0$ (3.10)
- $\frac{dF_{sCO2}}{dz} - 2\pi R_2 J_{CO2} = 0$ (3.11)
- $\frac{dF_{sCO}}{dz} - 2\pi R_2 J_{CO} = 0$ (3.12)
- $\frac{dF_{sH2}}{dz} - 2\pi R_2 J_{H2} = 0$ (3.13)
- $\frac{dF_{sN2}}{dz} - 2\pi R_2 J_{N2} = 0$ (3.14)
- $\frac{dF_{sH2O}}{dz} - 2\pi R_2 J_{CO} = 0$ (3.15)

3.3 PERMEATION RATE OF GASEOUS COMPONENTS THROUGH MEMBRANE

3.3.1 Permeation Rate through Porous Vycor Glass Membrane

In dense porous membranes diffusion of gaseous components depends on the structure of the membrane as well as the pores in the membrane. In such membranes the gaseous components diffuses into the voids and follows a tortuous path with is greater than the thickness d of the membrane, by a factor τ called tortuosity. The separation of gaseous component through a membrane is governed by the following four processes:

1. Knudsen diffusion


भारतीय प्रौद्योगिकी संस्थान रुड़की
श्रमं विना न किमपि साध्यम्
SHRAMAM VINA NA KIMAPI SADHYAM
INDIAN INSTITUTE OF TECHNOLOGY ROORKEE

2. Surface diffusion
3. Capillary condensation
4. Molecular sieving

But the separation through a porous membrane can occur with the help of more than one phenomenon depending upon:

- chemical nature of the permeating molecules
- the size of permeating molecules
- pore size of the membrane,
- the membrane material,
- pore size distribution,
- temperature,
- pressure and
- the interaction among the gaseous molecule being separated.

In the present study we are using a mesoporous membrane in which the governing separation mechanism is assumed to be the Knudsen diffusion. In Knudsen diffusion it is assumed that the mean free path of the molecules is greater than the diameter of the pore and the interaction/collisions occur primarily between the gaseous molecules and the walls of pores rather than between gaseous molecules. The membrane permeation flux for any component i through the membrane can be written as:

$$J_i = D_i(P_{ti} - P_{si}) \tag{3.16}$$

Where the Knudsen diffusivity D_i is given by

$$D_i = \frac{2r\varepsilon}{3\tau RTd}\sqrt{\frac{8000RT}{\pi M_i}} \tag{3.17}$$


भारतीय प्रौद्योगिकी संस्थान रुड़की
श्रम विना न किमपि साध्यम्
SHRAMAM VINA NA KIMAPI SADHYAM
INDIAN INSTITUTE OF TECHNOLOGY ROORKEE

3.3.2 Permeation Rate through Pd/Pd Alloy Composite Dense Permeable Membrane

The Pd/Pd-alloy dense membrane is selectively permeable to Hydrogen as compared to other gases. The permeability's J_i or the permeation rate of all other components other than hydrogen through Pd or Pd alloy composite membranes is 0. In case of these membranes the diffusion of gases is not dependent on the actual structure of the membrane film. In Pd/Pd-alloy composite membranes the diffusion of gas through membranes is assumed to follow Fick's law as the gas is dissolved in the membrane film to form a homogenous medium(more or less).

The permeability coefficient A_0 for any component i is defined as moles of gaseous component i diffusing per second s per m^2(crossectional area) through the membrane of 1 m thickness and a pressure of 1atm. Thus applying Ficks law, the permeation flux in terms of permeability coefficient A_0 for H_2 through Pd or Pd alloy composite membranes for 50μm membrane thickness can be written as [Gallucci et al. 2004]:

$$J_{H2} = A_0 e^{\frac{E_a}{RT}}(\sqrt{P_{tH2}} - \sqrt{P_{sH2}}) \tag{3.18}$$

$E_a = 29.16\ kj/mol$

$A_0 = 7.06 * 10^{-4}\ mol\, m^{-2} s^{-1} Pa^{-0.5}$

3.4 KINETIC MODELS

For the modelling process, it is one of the most important steps to know the reaction kinetics. Based on literature review done, it is evident the type of support has a significant effect on the activity of the catalyst. As a result the reaction kinetics is affected by the metal and also by the support. Various studies done indicate that supported nickel and supported noble metal catalysts give good catalytic performance in terms of CH_4 conversion and synthetic gas selectivity. Many researchers have reported kinetics for dry reforming of methane on various catalysts. The kinetics are different as the results are based on different operating conditions and rate determining steps. In order to investigate the effect of type of catalyst on kinetics and simulation results, two catalysts Rh/Al_2O_3 (noble) and Ni/Al_2O_3 (non-noble with 10.6wt% Ni) has been selected. The kinetics of reforming reaction along with reverse water gas shift reaction is to be studied on these catalysts.


भारतीय प्रौद्योगिकी संस्थान रुड़की
श्रमं विना न किमपि साध्यम्
SHRAMAM VINA NA KIMAPI SADHYAM
INDIAN INSTITUTE OF TECHNOLOGY ROORKEE

Various models when fitted on experimental data showed that the models based on stepwise mechanism were in best agreement and the developed models suggested that there was no single rate determine step. The models are usually based on Langmuir- Hinshelwood or Eley-Rideal mechanism as the experimental data are found to be consistent with them. The kinetic models proposed by researchers on the above mentioned catalysts are discussed in the following subsections.

3.4.1 Kinetics on Rh/Al_2O_3 catalyst

Richardson and Paripatyadar(1990) found out that $Rh/\Upsilon Al_2O_3$ was effective catalyst for dry reforming of methane (DRM) at low feed ratios. In the temperature range of 600-800^{0}C no carbon deposition was found. Rate expression for reforming of methane and RWGS reactions were determined on the basis of kinetic experiment done on 0.5wt% $Rh/\Upsilon Al_2O_3$ catalyst. Both the reverse reaction and the effect of external and internal diffusion were considered in the model development. Kinetic measurements were made with a tubular fixed bed reactor. The operating pressure was 1 atm and operating temperatures were 873, 923, and 973 K. Carbon dioxide partial pressure varied from 0.25 to 0.55 atm and that of methane from 0.085 to 0.451 atm. 38 runs were carried out in which the feed ratio (CH_4/CO_2) range varied from 1 to 5. Feed flow rate was limited to 200cm^3. The data were tested with rate equation suggested by Langmuir- Hinshelwood redox mechanisms. First the rate for the forward reforming and RWGS reaction were found by linear regression analysis. It was found that the reverse water gas shift reaction was not in equilibrium as its equilibrium constant was almost 10 times more than that estimated in kinetic reforming experiments. Therefore a rate equation for the RWGS reaction was necessary. The kinetic rate expressions for the forward reforming reaction and forward RWGS reaction were:

$$r_{1f} = \frac{k_1 K_{CH4} K_{CO2} p_{CH4} p_{CO2}}{(1+K_{CO2}p_{CO2}+K_{CH4}p_{CH4})^2} \tag{3.19}$$

$$r_{2f} = k_2 p_{CO2} \tag{3.20}$$

The temperature dependence of the constants were found to be


भारतीय प्रौद्योगिकी संस्थान रुड़की
श्रमं विना न किमपि साध्यम्
SHRAMAM VINA NA KIMAPI SADHYAM
INDIAN INSTITUTE OF TECHNOLOGY ROORKEE

$$k_1 = 1290e^{\frac{-102065}{RT}} \quad gmolg_{cat}^{-1}s^{-1} \tag{3.21}$$

$$K_{CO2} = 2.61 * 10^{-2}e^{\frac{37641}{RT}} \text{ atm}^{-1} \tag{3.22}$$

$$K_{CH4} = 2.60 * 10^{-2}e^{\frac{40684}{RT}} \text{ atm}^{-1} \tag{3.23}$$

The overall or the net rate equations were determined by considering the reverse rate expressions for reforming and RWGS reaction. Reverse rate expressions were determined by the addition of a term to the forward rate equation, and the concept that at equilibrium net rate approaches zero was used. Thus the net rates of reactions obtained were:

$$r_1 = r_{1f}\frac{1-(p_{CO}p_{H2})^2}{K_1 p_{CH4}p_{CO2}} \tag{3.24}$$

$$r_2 = r_{2f}\frac{1-p_{CO}p_{H2O}}{K_2 p_{H2}p_{CO2}} \tag{3.25}$$

Where r_{1f} and r_{2f} represent the forward reaction rates of reforming reaction and RWGS reaction respectively and K_1 and K_2 are the respective equilibrium constants.

3.4.2 Kinetics on Ni/Al_2O_3 (10.6 wt% Ni) Catalyst:

Becerra et al., carried out the kinetic analysis of dry reforming of methane over stable Ni/Al_2O_3 (10.6 wt% Ni) catalyst in a fixed bed reactor. The kinetics was studied in the range of 773-873 K, at normal pressure and various feed molar ratios (CO_2/CH_4: 1, 2, 3, 4). Also molar feed ratio H_2/CH_4: 0.4 was used to prevent re-oxidation and therefore deactivation of catalyst.

In order to estimate the kinetic parameters, 78 experiments were conducted, in which conversion of methane and carbon dioxide was calculated. Models based on Langmuir-Hinshelwood and Eley-Rideal mechanism were proposed and tested. Eley-Rideal type model described adequately the main reaction of the Carbon dioxide reforming of methane. The influence of the reverse water-gas shift reaction was also included. Assumption used in the model development is the CH_4 is non-dissociatively adsorbed on the catalyst surface in an adsorption equilibrium. The reaction of the adsorbed species with carbon dioxide from the

भारतीय प्रौद्योगिकी संस्थान रुड़की
श्रमं विना न किमपि साध्यम्
SHRAMAM VINA NA KIMAPI SADHYAM
INDIAN INSTITUTE OF TECHNOLOGY ROORKEE

gas phase leading directly to the products is considered the rate-determining step. The kinetic parameters determined are statistically important and comparable with those reported in the literature. The heterogeneous models considered for the reverse water gas shift reaction resulted in worse fits, so a simplified equation based on overall reaction for RWGS reaction was proposed. The kinetic rate expressions for the reforming reaction and RWGS reaction are as follows:

$$r_1 = k_3 K_3 \frac{p_{CH4} p_{CO2} - \frac{p_{CO}^2 p_{H2}^2}{K_1}}{1 + K_{11} p_{CH4}} \tag{3.26}$$

$$r_2 = k_4 (p_{CO2} p_{H2} - \frac{p_{CO} p_{H2O}}{K_2}) \tag{3.27}$$

Where r_1 is rate of reforming reaction and r_2 is rate of RWGS reaction. The temperature dependence of the constants was given as:

$$k_3 = 7.13 * 10^5 e^{\frac{[(-10.7 \pm 1.1) * 10^4]}{RT}} \quad (\text{mol g}^{-1}\ \text{bar}^{-1}\ \text{hr}^{-1}) \tag{3.28}$$

$$k_4 = 15.92 e^{\frac{[(-64.8 \pm 38.0) * 10^3]}{RT}} \quad (\text{mol g}^{-1}\ \text{bar}^{-1}\ \text{hr}^{-1}) \tag{3.29}$$

$$K_{11} = 4.01 * 10^{-4} e^{\frac{[(74.6 \pm 26.0) * 10^3]}{RT}} \quad (\text{bar}^{-1}) \tag{3.30}$$

3.5 THERMODYNAMIC ANALYSIS:

3.5.1 Equilibrium constant

The relation between the reaction equilibrium constant and the temperature for general gas phase reaction is given as [Smith et al.(2001),] :

$$lnK = -\frac{\Delta H_{298}}{RT} + \frac{\Delta a1}{R} lnT + \frac{\Delta b1}{2R} T + \frac{\Delta c1}{6R} T^2 + I \tag{3.31}$$

भारतीय प्रौद्योगिकी संस्थान रुड़की
श्रमं विना न किमपि साध्यम्
SHRAMAM VINA NA KIMAPI SADHYAM
INDIAN INSTITUTE OF TECHNOLOGY ROORKEE

Where I is the integration constant and its value can be determined by the value of equilibrium constant at a single temperature. The main six reactions which occur in dry reforming of methane are presented in section 1.2.4. The variation of equilibrium constant with temperature for the six reactions considered can be obtained by using the above equation. The derived equations are:

Dry reforming reaction:

$$lnK_1 = -\frac{28728.05}{T} + 5.694lnT - \frac{3.1785}{10^3}T - \frac{.00229}{10^6}T^2 + \frac{.0722}{10^9}T^3 + \frac{63044}{T^2} - 4.64 \quad (3.32)$$

RWGS reaction:

$$lnK_2 = -\frac{5906.303}{T} - 1.86lnT + \frac{2.7}{10^4}T + \frac{58200}{T^2} + 18.08 \quad (3.33)$$

Methane cracking reaction:

$$lnK_3 = \frac{7395.96}{T} + 6.56lnT - 0.00373T - 35000T^2 - 33.3856 \quad (3.34)$$

Boudouard reaction:

$$lnK_4 = \frac{20139}{T} + 0.475lnT - 0.00351T - \frac{98100}{T^2} - 27.8 \quad (3.35)$$

CO reduction reaction:

$$lnK_5 = \frac{15666}{T} - 1.385lnT + 0.0006615T - \frac{39900}{T^2} - 7.026 \quad (3.36)$$

CO_2 reduction reaction:

$$lnK_6 = \frac{10045}{T} - 3.245lnT + 0.0008815T - \frac{39650}{T^2} - 11.6 \quad (3.37)$$

According to the thermodynamic principles when the Gibbs free energy change of reaction (ΔG^0) is negative, the reaction is spontaneous and when ΔG^0 is positive, the reaction is thermodynamically limited/non spontaneous. For negative value of Gibbs free energy change


भारतीय प्रौद्योगिकी संस्थान रुड़की
श्रमं विना न किमपि साध्यम्
SHRAMAM VINA NA KIMAPI SADHYAM
INDIAN INSTITUTE OF TECHNOLOGY ROORKEE

of reaction (ΔG^0) higher values of K indicates that a spontaneous process/reaction is more feasible to occur. Fig. illustrated the variation of equilibrium constant K for all the six reactions with various temperatures in order to determine the extent to which the reaction occurs. The figure indicates that the equilibrium constants for the strongly endothermic CO_2 reforming reaction and CH_4 cracking reaction increase rapidly with increase in temperature as compared to the equilibrium constant for RWGS reaction which increases slowly with temperature as it is mildly endothermic. The other three reaction that are Boudouard reaction, CO reduction reaction and CO_2 reduction reaction are highly exothermic reactions so their equilibrium constant decrease rapidly with increase in temperature. The above findings lead to the conclusion that if the CO2 reforming of methane is carried out at higher temperature the three coke formation reactions namely Boudouard reaction, CO reduction reaction and CO_2 reduction reaction can be excluded from the reaction scheme. Thus on the basis thermodynamic analysis of equilibrium constants of reactions at various temperature an operating temperature range 873-1500K has been considered for the thermodynamic analysis.

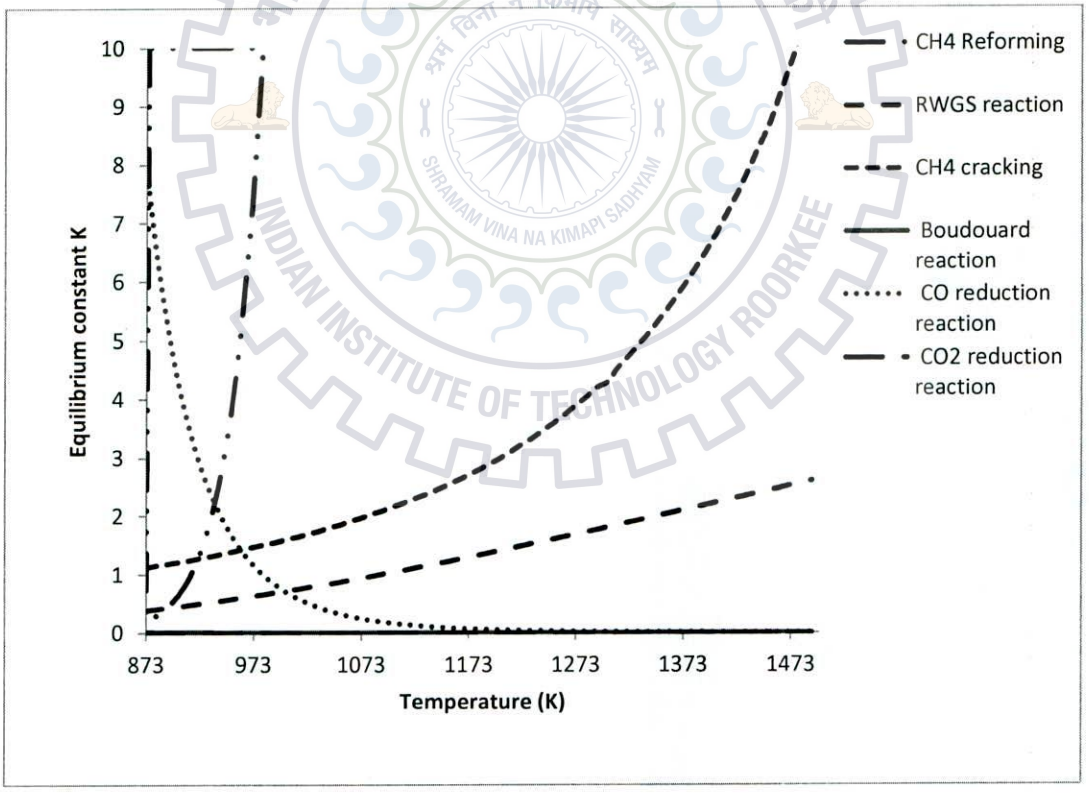

Fig 3.3 Equilibrium constants of reactions involving in dry reforming of methane at different temperatures and a pressure of 1 atm.


भारतीय प्रौद्योगिकी संस्थान रुड़की
श्रमं विना न किमपि साध्यम्
SHRAMAM VINA NA KIMAPI SADHYAM
INDIAN INSTITUTE OF TECHNOLOGY ROORKEE

3.5.2 Carbon formation boundary

Thermodynamic analysis is an important tool to identify and define the conditions for the potential carbon formation on the catalyst surface by reactions. Gibbs free energy minimization approach was used to estimate the conditions were the carbon formation will be thermodynamically unfavourable. The thermodynamic calculations were carried out using aspen plus. Aspen Plus is process simulation software which uses "basic engineering relationships, such as mass and energy balances, and phase and chemical equilibrium". Gibbs reactor is used to obtain the equilibrium compositions of the products.

The reactor RGibbs

This is the only Aspen Plus block that will deal with solid-liquid-gas phase equilibrium. It is useful when reactions occurring are not known or are high in number due to many components participating in the reactions. The concept of Gibbs free minimization is used for calculation. Chemical equilibria can be calculated between any number of conventional solid components and the fluid phases. RGibbs calculates the amount of solid if present at equilibrium. The different steps involved in ASPEN PLUS for simulating RGibbs reactor are:

In setup specification choosing stream class followed by entering all the reactants and all possible products and specifying their type i.e; conventional, non-conventional or pure solid. Then the base method is chosen and the stream specifications are entered like inlet temp, pressure, flow rate and feed fraction of components. Then the reactors conditions like pressure and temp/heat duty are entered.

On the basis of these inputs we obtain equilibrium product compositions(including solid compositions) and also by the use of calculator block(with some FORTRAN code) and sensitivity analysis tool we can obtain conversion, ratio, selectivity profiles, as per our requirement.

3.6 SOLUTION PROCEDURE

To study the dry reforming of methane, analysis was carried out in four different reactor configurations. The two configurations are of membrane reactors and the other two are fixed bed reactors. One membrane reactor (MR1) is packed with supported Rh metal based catalyst and equipped with porous vycor glass membrane. The vycor glass membrane is permeable to all gaseous components. The other membrane reactor (MR2) is packed with supported Ni

भारतीय प्रौद्योगिकी संस्थान रुड़की
श्रमं विना न किमपि साध्यम्
SHRAMAM VINA NA KIMAPI SADHYAM
INDIAN INSTITUTE OF TECHNOLOGY ROORKEE

metal based catalyst and equipped with hydrogen permeable dense Pd alloy membrane. The first fixed bed reactor (FBR1) is packed with supported Rh metal based catalyst. And the other fixed bed reactor (FBR2) is packed with supported Ni metal based catalyst. The feed to all the reactors is CH_4, CO_2 and N_2(diluent). N_2 is also used as a sweep gas in permeation zones.

The model equations for the membrane reactor and the fixed bed reactor are presented in sub section (3.2.1) and (3.2.2). In the present study the four carbon formation reactions have not been considered. Therefore the model equations (3.2)-(3.7) and (3.10)-(3.15) have been modified according by setting $r_3 = r_4 = r_5 = r_6 = 0$. The operating and boundary conditions are presented in the table 3.1 as the boundary conditions are given at z=0, so the given ordinary differential equations constitute initial value problems. In order to simulate the reactors, the model equations 12 for membrane reactor and 6 for fixed bed reactor are solved simultaneously in MATLAB-7b using ODE solver tool. For analysing the performance of the reactors following definitions for the equilibrium conversions of reactants, the yield and selectivity of products (H_2 or CO), partial pressures of gaseous components are used:

Percent methane conversion: (FBR1, FBR2 & MR2)

$$= \frac{F^0_{tCH4} - F_{tCH4}}{F^0_{tCH4}} \tag{3.38}$$

Percent methane conversion: (MR1)

$$= \frac{F^0_{tCH4} - (F_{tCH4} + F_{sCH4})}{F^0_{tCH4}} \tag{3.39}$$

Hydrogen Selectivity : (FBR1 & FBR2)

$$= \frac{F_{tH2}}{F_{tH2} + F_{tCO} + F_{tH2O}} \tag{3.40}$$

Hydrogen Selectivity : (MR2)

$$= \frac{F_{tH2} + F_{sH2}}{F_{tH2} + F_{tCO} + F_{tH2O} + F_{sH2}} \tag{3.41}$$


भारतीय प्रौद्योगिकी संस्थान रुड़की
श्रमं विना न किमपि साध्यम्
SHRAMAM VINA NA KIMAPI SADHYAM
INDIAN INSTITUTE OF TECHNOLOGY ROORKEE

Hydrogen Selectivity : (MR1)

$$= \frac{F_{tH2}+F_{sH2}}{F_{tH2}+F_{tCO}+F_{tH2O}+F_{sH2}+F_{sCO}+F_{sH2O}} \quad (3.42)$$

CO Selectivity: (FBR1 & FBR2)

$$= \frac{F_{tCO}}{F_{tH2}+F_{tCO}+F_{tH2O}} \quad (3.43)$$

CO Selectivity : (MR2)

$$= \frac{F_{tCO}}{F_{tH2}+F_{tCO}+F_{tH2O}+F_{sH2}} \quad (3.44)$$

CO Selectivity : (MR1)

$$= \frac{F_{tCO}+F_{sCO}}{F_{tH2}+F_{tCO}+F_{tH2O}+F_{sH2}+F_{sCO}+F_{sH2O}} \quad (3.45)$$

Yield of H_2: (FBR1 & FBR2)

$$= \frac{F_{tH2}}{F^0_{tCH4}} \quad (3.46)$$

Yield of H_2: (MR1 & MR2)

$$= \frac{F_{tH2}+F_{sH2}}{F^0_{tCH4}} \quad (3.47)$$

Yield of CO: (FBR1, FBR2 & MR2)

$$= \frac{F_{tCO}}{F^0_{tCH4}} \quad (3.48)$$

Yield of CO: (MR1)

$$= \frac{F_{tCO}+F_{sCO}}{F^0_{tCH4}} \quad (3.49)$$

भारतीय प्रौद्योगिकी संस्थान रुड़की
श्रमं विना न किमपि साध्यम्
SHRAMAM VINA NA KIMAPI SADHYAM
INDIAN INSTITUTE OF TECHNOLOGY ROORKEE

H_2/CO Ratio:

$$= \frac{yield\ of\ H_2}{yield\ of\ CO} \tag{3.50}$$

F_{ti}^0 molar flow rate of ith component at inlet of reactor. (mol/s)

F_{ti} molar flow rate of ith component at outlet of reactor. (mol/s)

Partial pressures

The partial pressure of any i^{th} component on the tube side(reaction zone) for the reactor both fixed bed and membrane bed reactor is given as:

$$P_{ti} = \frac{F_{ti}}{\sum_{i=1}^{6} F_{ti}} P_{tT} \tag{3.51}$$

For the shell side(permeation zone) of the membrane reactor the partial pressure of any i^{th} component is given as:

$$P_{si} = \frac{F_{si}}{\sum_{i=1}^{l} F_{si}} P_{sT} \tag{3.52}$$

In case when vycor glass membrane is used, as it is permeable to all the components so the number of components on permeate side is six so l=6. For palladium dense membrane l=2 as it is only permeable to hydrogen so on permeate side we have only two components, nitrogen(the sweep gas) and hydrogen.

3.6.1 Operating Conditions (for thermodynamic analysis)

- Total moles of reactant (CH_4 + CO_2) =6 moles
- Pressure = 1 atm.
- Temperature range: 873-1500 K.*
- CO_2/CH_4 ratio varied between 1 and 3.
- H_2 in feed varied from 0- 10%
- Possible products considered are:


भारतीय प्रौद्योगिकी संस्थान रुड़की
श्रमं विना न किमपि साध्यम्
SHRAMAM VINA NA KIMAPI SADHYAM
INDIAN INSTITUTE OF TECHNOLOGY ROORKEE

1) CH_4	2) H_2
3) CO	4) H_2O
5) CO_2	6) Carbon

* The selection of operating temperature and coke formation reactions has been carried out on the basis of thermodynamic analysis of equilibrium constants of reactions at various temperature and the operating temperature greater >=873 K has been selected to maintain the catalyst activity, and to achieve high conversion of CH_4 .

3.6.2 Boundary and Operating Conditions (for FBR1, FBR2, MR1 & MR2)

The values for the parameters to be used in simulation have been taken from previous experimental studies of Gallucci et al. (2008) and Prabhu et al (2008).

Table 3.1
Parameter value used in the simulation of the reactors.

Parameter	Value
z	0.04 m
P_t	1 atm
P_s	1 atm
R	8.314 J/mol/K
R_1	.004 m
R_2 (MR1)	.005 m
R_2 (MR2)	.00405 m
R_3	.007 m
ε	0.6
τ	3.0
R	4.0 nm
d (MR1)	1.0 mm
d (MR2)	50 µm
F^0_{tCH4}	24 µmol/s


भारतीय प्रौद्योगिकी संस्थान रुड़की
श्रमं विना न किमपि साध्यम्
SHRAMAM VINA NA KIMAPI SADHYAM
INDIAN INSTITUTE OF TECHNOLOGY ROORKEE

Parameter	Value
F^0_{tCO2}	24 µmol/s
F^0_{tN2}	27 µmol/s
F^0_{sCH4}	0 µmol/s
F^0_{sCO2}	0 µmol/s
F^0_{sN2}	7 µmol/s

Using the above mentioned operating conditions in the next chapter first the results from the thermodynamic analysis have been presented and on the basis of these results optimum temperature and per cent of H_2 to be added to feed has been selected. Then the model equations for FBR1, MR1, FBR2 and MR2 have been solved using the operating and boundary conditions presented in table 3.1 together with the results obtained from thermodynamic analysis.

भारतीय प्रौद्योगिकी संस्थान रुड़की
श्रमं विना न किमपि साध्यम्
SHRAMAM VINA NA KIMAPI SADHYAM
INDIAN INSTITUTE OF TECHNOLOGY ROORKEE

CHAPTER 4

RESULTS AND DISSCUSSIONS

4.1 CARBON FORMATION BOUNDARIES

As discussed in the section (3.5.1) methane cracking reaction is the prominent/favourable carbon formation reaction in the temperature range of 873-1500K. Different amount of carbon deposition takes place depending upon the feed CO_2/CH_4 ratio, operating temperature and operating pressure. The thermodynamic analysis has been carried out to find the optimum operating conditions for the reactor operation, so as to minimize carbon formation and at the same time obtain H_2/CO ratio that desirable for Fisher-Tropsch synthesis.

4.1.1 Effect of Temperature and CO_2/CH_4 Ratio on Equilibrium Reactant Conversion and Product Distribution.

Figures (4.1) – (4.7) represent the trends for methane conversion, carbon dioxide conversion, carbon formation, H_2 yield, H_2 selectivity, H_2/CO ratio and CO selectivity as a function of temperature at different CO_2/CH_4 ratio. As seen from the figures, the CO_2/CH_4 reactant ratio and reaction temperature had a considerable influence on the equilibrium of the reactants conversion, equilibrium composition of the products and solid carbon formation. It is noteworthy from fig (4.1) that at a particular temperature as the CO_2/CH_4 ratio increase from 1-3 the methane conversion increases, since CH_4 acts as the limiting reactant. Also the methane conversion increases quickly with increase in temperature up to 1000K, after that the conversion increases smoothly towards 100% conversion. CO_2 conversion also increases with increasing temperature, as both reforming reaction and RWGS reaction responsible for CO_2 consumption are endothermic and are favoured at higher temperature.

From fig (4.5) we observe that carbon formation/deposition decreases with increase in temperature as higher temperature is a barrier for improving the exothermic reactions namely Boudouard reaction, CO reduction reaction and CO_2 reduction reaction which involved carbon formation. Also with increase in CO_2/CH_4 ratio from 1 to 3 carbon formation decreases as CH_4 becomes the limiting reactant and thus the main carbon formation reaction i.e. methane cracking reaction is not much involved in carbon formation. When CO_2/CH_4

भारतीय प्रौद्योगिकी संस्थान रुड़की
श्रमं विना न किमपि साध्यम्
SHRAMAM VINA NA KIMAPI SADHYAM
INDIAN INSTITUTE OF TECHNOLOGY ROORKEE

ratio is increased from 1-2, carbon formation is negligible beyond 1000K. While at CO_2/CH_4 ratio 3, carbon formation approaches zero at about 960K.

From fig (4.6) we see that the H_2 selectivity decreases with the increase in CO_2/CH_4 ratio. The reason for such a behaviour being that on increasing the feed CO_2/CH_4 ratio the methane becomes the limiting reactant and thus the production of H_2 by methane cracking reaction and reforming reaction decreases. Also for CO_2/CH_4 ratio >=2, we observe that at a temperature greater than 980K the H_2 selectivity decreases because of the RWGS reaction as Hydrogen is being consumed in the reaction.

Fig (4.3) shows the variation of H_2/CO ratio produced as a function of temperature and CO_2/CH_4 ratio, at a pressure of 1 atm. From the results obtained it is clear that at any CO_2/CH_4 ratio with increase in temperature the H_2/CO ratio decreases and attains a value near about 1. This represents that at higher temperatures the preferred reaction is the methane reforming reaction. And as we increase the CO_2/CH_4 feed ratio, at any particular temperature the H_2/CO ratio decreases. Thus, for H_2/CO ratio close to unity, increase in CO_2/CH_4 ratio from 1 to 3 decreases operating temperature from 1283K to 873K.

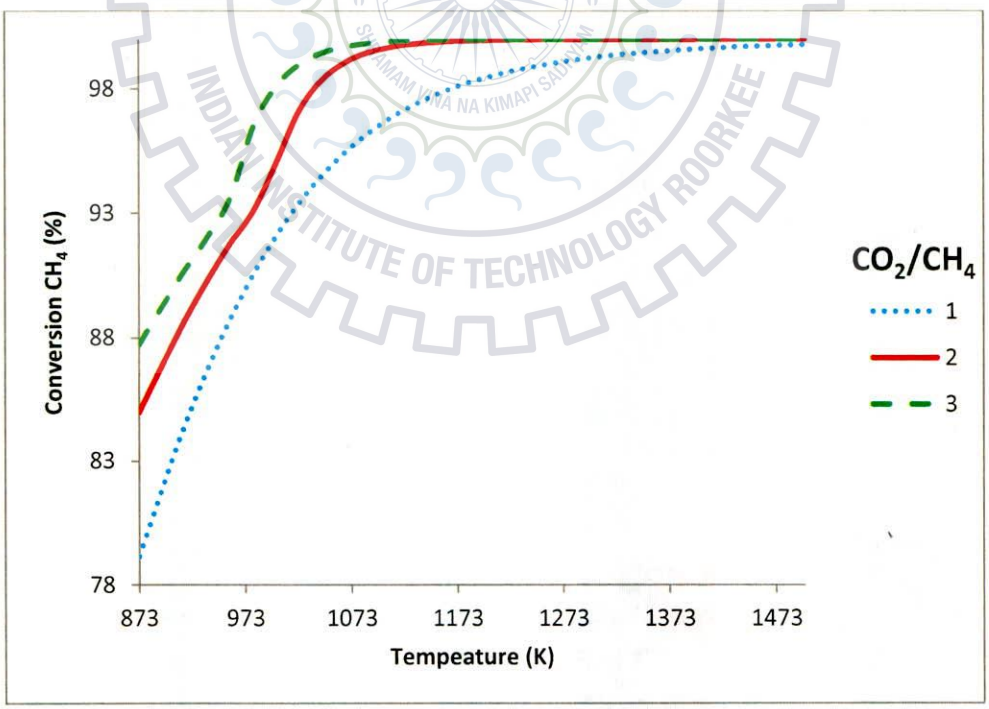

Fig 4.1 CH_4 equilibrium conversion as a function of temperature and CO_2/CH_4 ratio at 1 atm & $n(CH_4+CO_2)=6$ moles


भारतीय प्रौद्योगिकी संस्थान रुड़की
श्रमं विना न किमपि साध्यम्
SHRAMAM VINA NA KIMAPI SADHYAM
INDIAN INSTITUTE OF TECHNOLOGY ROORKEE

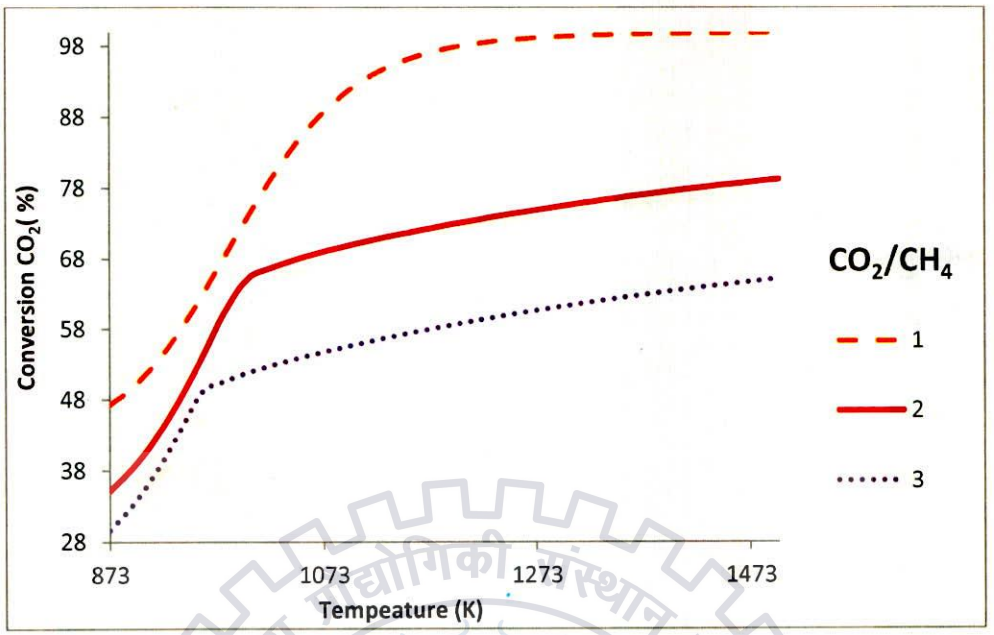

Fig 4.2 CO_2 equilibrium conversion as a function of temperature and CO_2/CH_4 ratio at 1 atm for n (CH_4+CO_2) = 6 moles

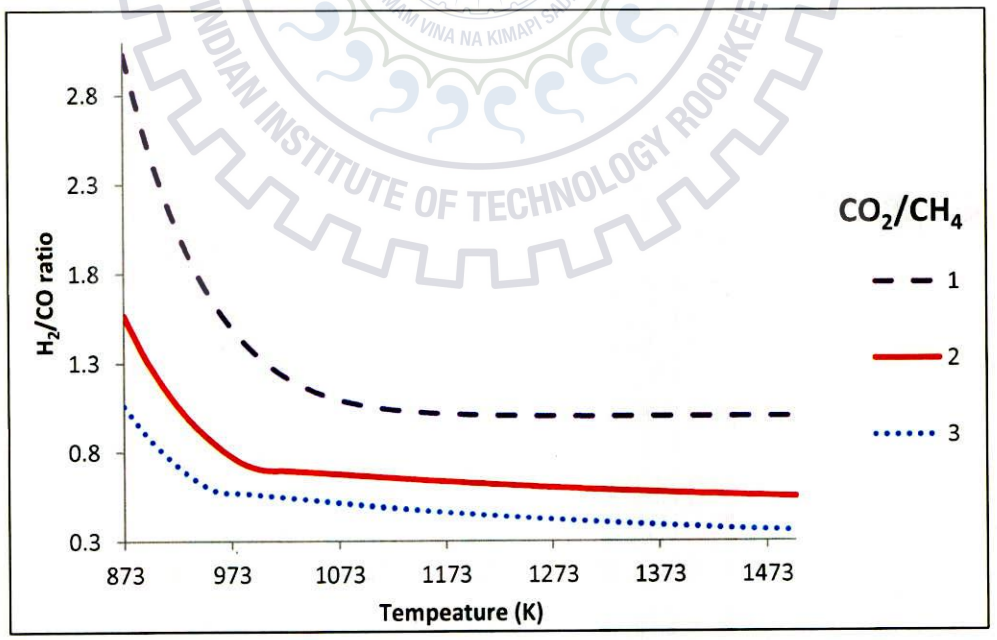

Fig 4.3 H_2/CO ratio as a function of temperature (873-1500 K) and CO_2/CH_4 ratio at 1 atm for n (CH_4+CO_2)=6 moles


भारतीय प्रौद्योगिकी संस्थान रुड़की
श्रमं विना न किमपि साध्यम्
SHRAMAM VINA NA KIMAPI SADHYAM
INDIAN INSTITUTE OF TECHNOLOGY ROORKEE

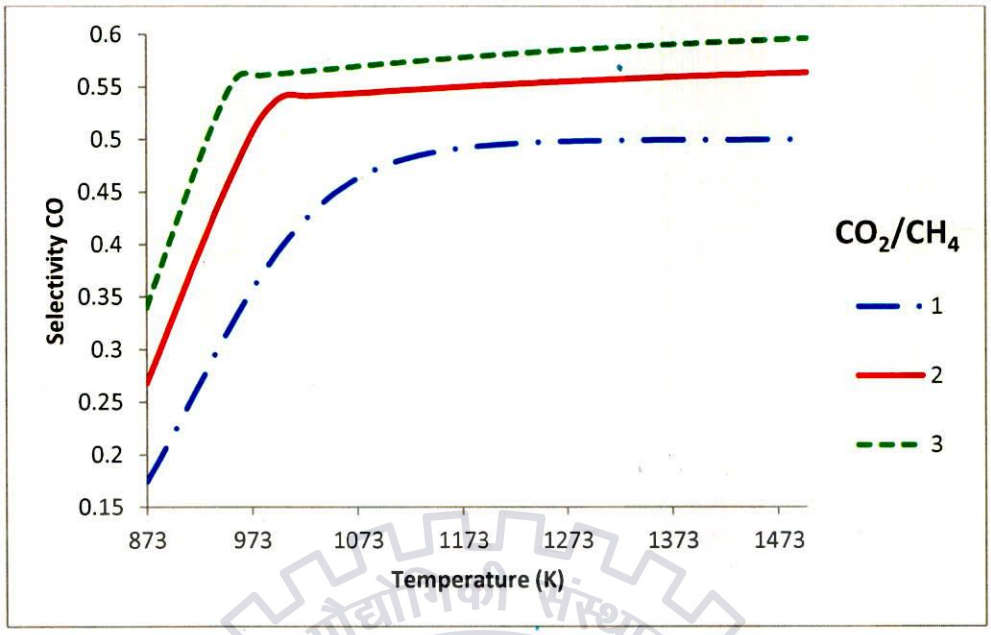

Fig 4.4: CO selectivity as a function of temperature (873-1500 K) and CO_2/CH_4 ratio at 1 atm for n (CH_4+CO_2)=6 moles

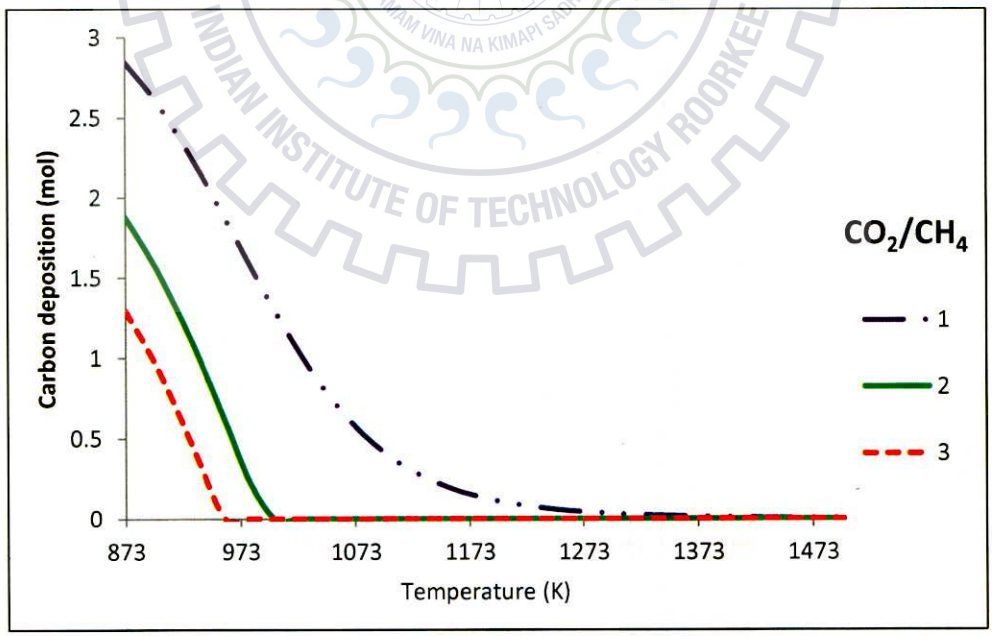

Fig 4.5 Moles of Carbon as a function of temperature and CO_2/CH_4 ratio at 1 atm for n (CH_4+CO_2)=6 mol.


भारतीय प्रौद्योगिकी संस्थान रुड़की
श्रम विना न किमपि साध्यम्
SHRAMAM VINA NA KIMAPI SADHYAM
INDIAN INSTITUTE OF TECHNOLOGY ROORKEE

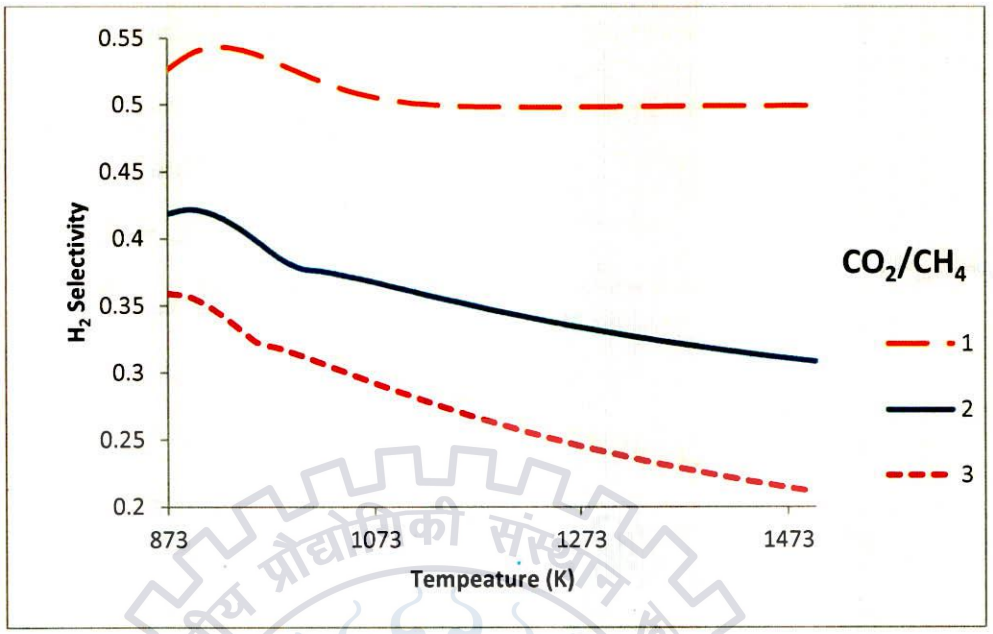

Fig 4.6 H_2 selectivity as a function of temperature and CO_2/CH_4 ratio at 1 atm for n (CH_4+CO_2)=6 moles

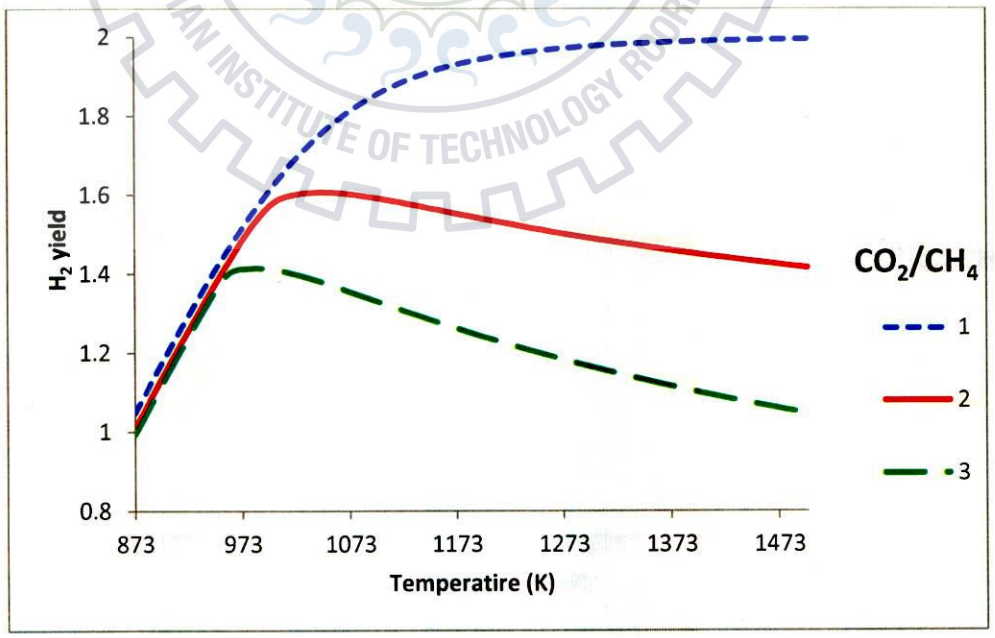

Fig 4.7 H_2 yield as a function of temperature and CO_2/CH_4 ratio at 1 atm for n (CH_4+CO_2)=6 moles


भारतीय प्रौद्योगिकी संस्थान रुड़की
श्रमं विना न किमपि साध्यम्
SHRAMAM VINA NA KIMAPI SADHYAM
INDIAN INSTITUTE OF TECHNOLOGY ROORKEE

4.1.2 Effect of Temperature and Hydrogen Addition on Equilibrium Reactant Conversion and Product Distribution.

In this section of thermodynamic analysis hydrogen in the feed was added in 1%, 5% and 10% of the total feed. The effect of H_2 addition on CH_4 conversion, carbon formation, hydrogen selectivity, hydrogen yield, CO selectivity and H_2/CO ratio has been investigated in the temperature range of 873-1500K. Fig (4.8) shows that at a particular temperature as the percentage of H2 increases in the feed the methane conversion decreases as both the methane conversion reactions that are methane reforming and cracking reactions are suppressed.

Considering the fig (4.10), we observe three important points. Firstly, selectivity of H2 increases with the increase in H_2 addition for CO_2/CH_4 ratio (1-3). Secondly, at a particular temperature and hydrogen concentration the selectivity decreases with increase in CO_2/CH_4 ratio. Thirdly, to obtain hydrogen selectivity of greater than 0.5 reduces the CO_2/CH_4 ratio to unity and excludes the 0% hydrogen addition for temperature greater than 1000K.

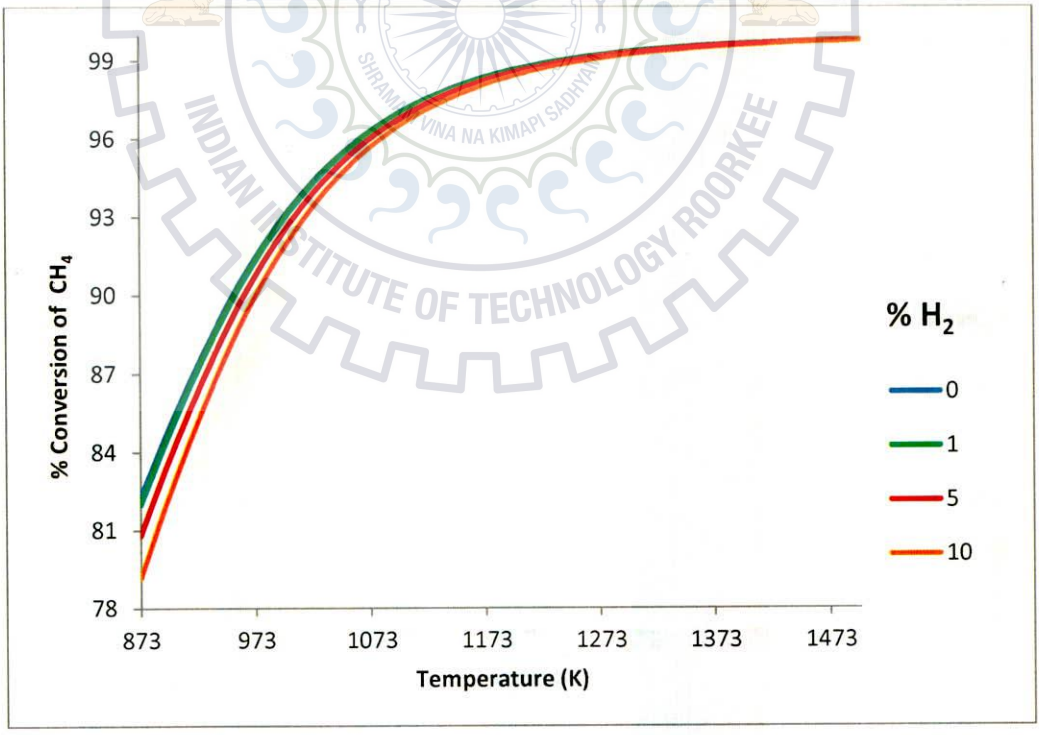

Fig 4.8 CH_4 equilibrium conversion as a function of temperature and % H_2 addition at CO_2/CH_4 =1, P= 1 atm & (CH_4+CO_2)=6 mol.


भारतीय प्रौद्योगिकी संस्थान रुड़की
श्रमं विना न किमपि साध्यम्
SHRAMAM VINA NA KIMAPI SADHYAM
INDIAN INSTITUTE OF TECHNOLOGY ROORKEE

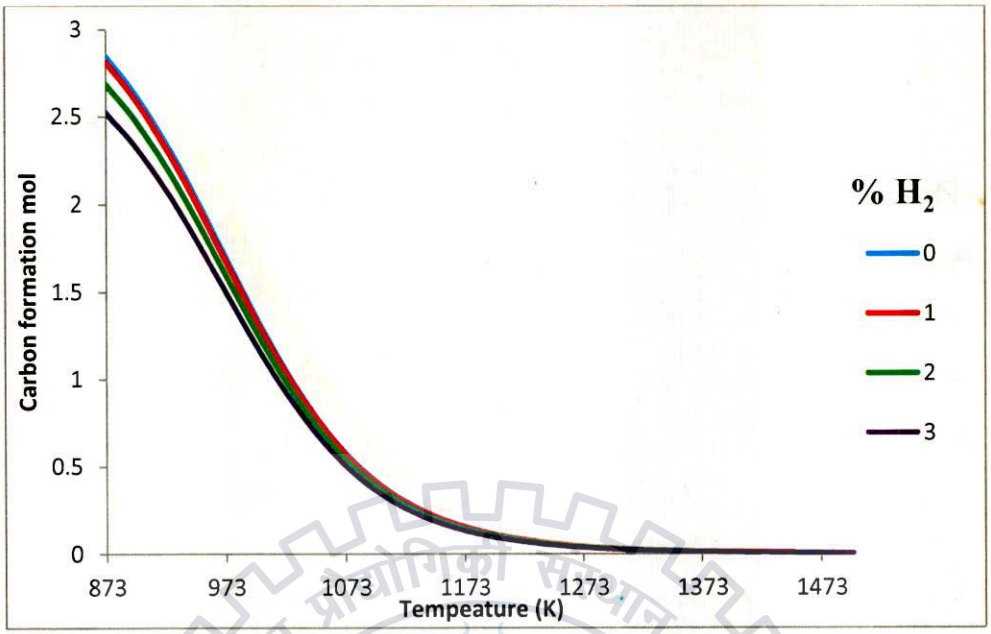

Fig 4.9 Moles of Carbon as a function of temperature and % H_2 addition at CO_2/CH_4 =1, P= 1 atm & (CH_4+CO_2)=6 mol.

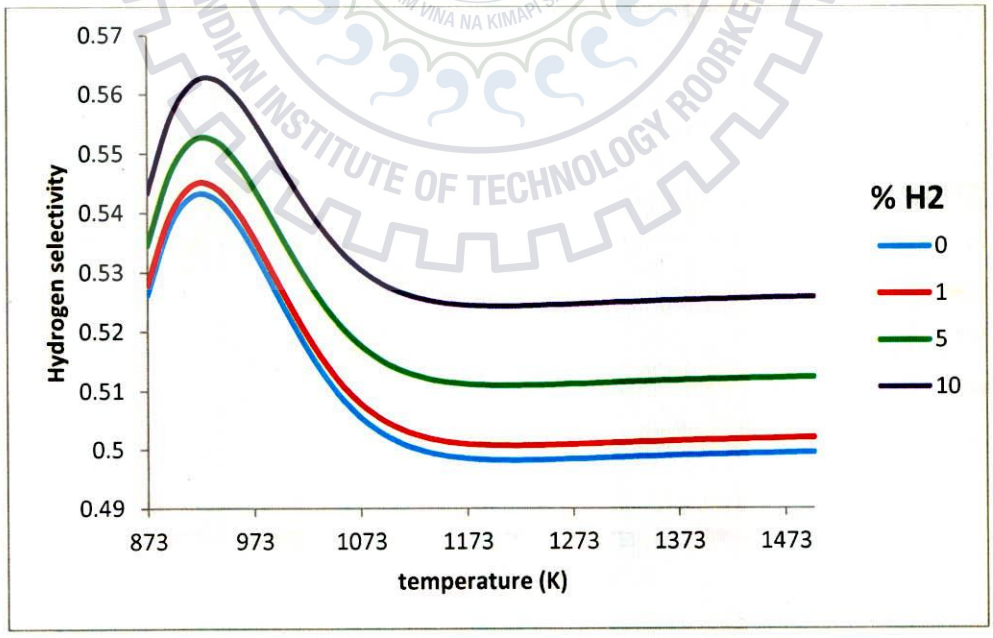

Fig 4.10 H_2 selectivity as a function of temperature and % H_2 addition at CO_2/CH_4 =1, P= 1 atm & (CH_4+CO_2)=6 mol.


भारतीय प्रौद्योगिकी संस्थान रुड़की
श्रमं विना न किमपि साध्यम्
SHRAMAM VINA NA KIMAPI SADHYAM
INDIAN INSTITUTE OF TECHNOLOGY ROORKEE

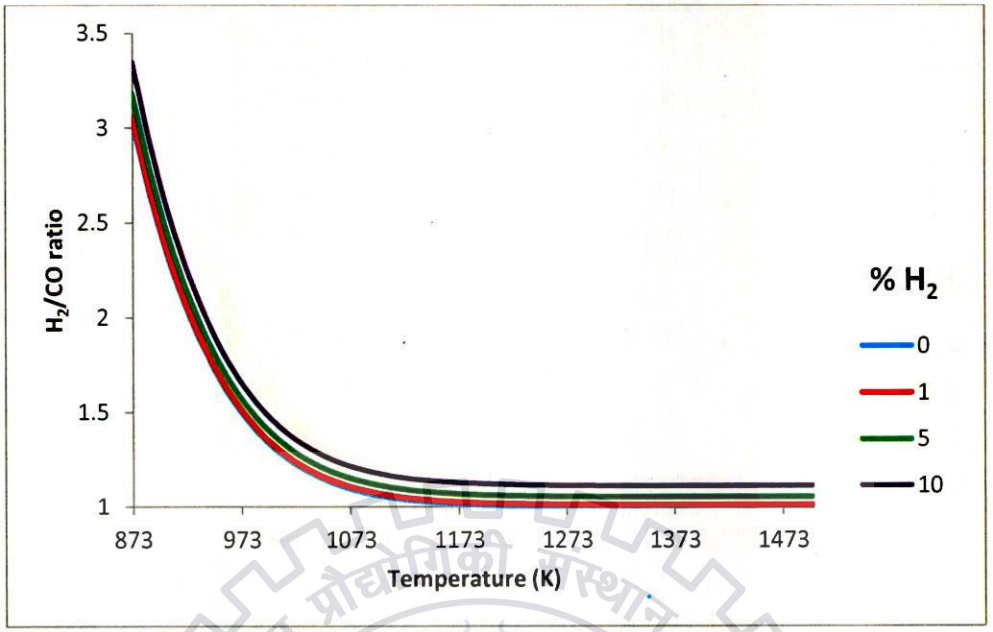

Fig 4.11 H_2/CO ratio as a function of temperature and % H_2 addition at CO_2/CH_4 =1, P= 1 atm & (CH_4+CO_2)=6 mol.

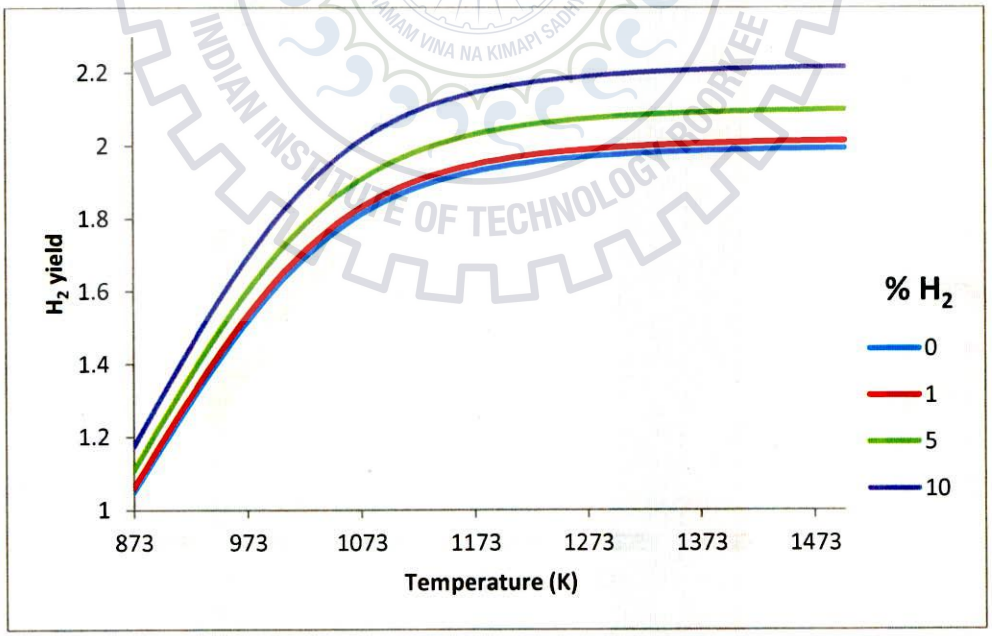

Fig 4.12 H_2 yield as a function of temperature and % H_2 addition at CO_2/CH_4 =1, P= 1 atm & (CH_4+CO_2)=6 mol.


भारतीय प्रौद्योगिकी संस्थान रुड़की
श्रमं विना न किमपि साध्यम्
SHRAMAM VINA NA KIMAPI SADHYAM
INDIAN INSTITUTE OF TECHNOLOGY ROORKEE

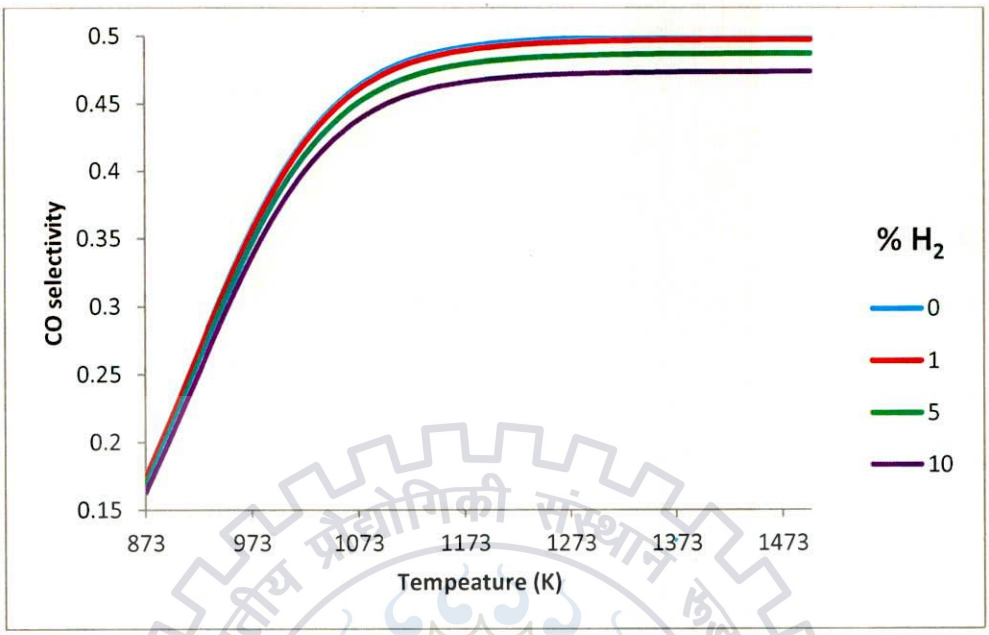

Fig 4.13 CO selectivity as a function of temperature and % H_2 addition at CO_2/CH_4 =1, P= 1 atm & (CH_4+CO_2)=6 mol.

From the results obtained it can be noticed that the stability of catalyst greatly increases with H_2 addition to feed. From fig (4.9) it can be noted that at any particular temperature as the percentage of H_2 increases in the feed Carbon formation decreases as higher percentage of H_2 in the feed suppresses the methane cracking reaction. For CO_2/CH_4 ratio of unity and at a temperature of about 1262K, the carbon formation reduces to less than 0.05 mol/s irrespective of hydrogen concentration in the feed. Also, when CO_2/CH_4 ratio is increased from 1 to 2, carbon formation is negligible beyond 1000K. While at CO_2/CH_4 ratio of 3, carbon formation approaches zero at 956K.

On the basis of various results obtained from thermodynamic analysis it can be concluded that carbon formation on the catalyst surface can be avoided by increasing the feed ratio from 1 to 3 and by operating at high temperature. But from the point view of the use of syngas in manufacture of industrial chemicals and particularly for Fisher-Tropsch process, syngas with H_2/CO ratio of unity is desirable and for that as evident from the results presented in table 4.1, at higher temperature the desirable CO_2/CH_4 feed ratios are less than 2.


भारतीय प्रौद्योगिकी संस्थान रुड़की
श्रम विना न किमपि साध्यम्
SHRAMAM VINA NA KIMAPI SADHYAM
INDIAN INSTITUTE OF TECHNOLOGY ROORKEE

Table 4.1

Minimum CH_4 conversion, carbon deposition and H_2/CO ratio as a function of temperature, percent hydrogen addition and CO_2/CH_4 feed ratio.

CO_2/CH_4	H_2/CO	Temperature range (K)	Conv of CH_4 (%)	Carbon Deposition (mol/s)	% H_2
1	<=1	1286-1500	99.2827793	0.03679	0
	<=1.5	973 -1285	91.3927602	1.693163	0
		975-1286	91.4015739	1.64665	1
		983-1500	91.4295275	1.466509	5
		722-1500	91.5859863	1.232115	10
	<=2	925-972	87.5252427	2.322535	0
		654-974	87.2978716	2.098646	1
		933-982	87.2978716	2.098646	5
		668-721	87.0378578	1.880844	10
	<=2.5	896-924	84.6953918	2.640621	0
		624-653	84.5640575	2.60129	1
		902-932	84.1200913	2.43514	5
		636-667	83.5964542	2.22278	10
	<=3	875 to 895	82.4531969	2.82877	0
		602-623	81.6180294	2.630245	1
		880-901	81.6180294	2.630245	5
		613-635	80.8151247	2.425284	10
2	<=1	931-1500	92.0966962	1.096094	0
		993-1500	92.0134852	1.05343	1
		942-1500	91.7344415	0.868898	5
		954-1500	91.4233717	0.633378	10
	<=1.5	878-930	88.7133821	1.824476	0
		880-992	88.5651055	1.785083	1
		887-941	87.8791094	1.638387	5
		896-953	86.9830347	1.451764	10
3	<=1	880-1500	91.6896671	1.209108	0
		883-1500	91.5473518	1.164188	1
		892-1500	90.8068542	1.019184	5
		904-1500	89.8821116	0.824084	10

So the optimum operating conditions considering CH_4 conversion, carbon deposition, H_2 selectivity and H_2/CO ratio are:

CO_2/CH_4 feed ratio of 1:1, 5% H_2 addition and operating temperature of 1180K.

भारतीय प्रौद्योगिकी संस्थान रुड़की
श्रमं विना न किमपि साध्यम्
SHRAMAM VINA NA KIMAPI SADHYAM
INDIAN INSTITUTE OF TECHNOLOGY ROORKEE

4.2 MODEL VALIDATION FOR FIXED BED AND MEMBRANE REACTOR

4.2.1 Ni based catalyst (Ni/Al_2O_3)

The mathematical models for dry reforming of methane have been validated on the basis of percentage methane conversion, carbon dioxide conversion and H_2/CO ratio in FBR 2. For this purpose, the experimental studies of Kang et al. (2011) on methane dry reforming reaction in fixed bed reactor. Kang et al. (2011) carried out dry reforming in a fixed bed reactor (8 mm ID, 500 mm height) using nickel supported catalyst with core/shell structures of Ni/Al_2O_3 and tested for dry reforming of methane (DRM) to produce hydrogen and carbon monoxide. reaction was carried out in temperature ranging from 700°C to 800°C at atmospheric pressure with a total flow rate of 50 ml/min of mixed gasses of CH_4:CO_2:He=1:1:1. In the present study the, the model equations described in chapter 3 have been solved at same operating conditions as used by Kang et al. (2011). Table 4.2 compares the model predictions with experimental results.

Table 4.2
Validation of model results of fixed bed reactor with experimental results (Kang et al. 2011)

Temperature (^{0}C)	Experimental results for FBR2			Model results for FBR2			Error		
	% CH_4 conversion	% CO_2 conversion	H_2/CO ratio	% CH_4 conversion	% CO_2 conversion	H_2/CO ratio	% CH_4 conversion	% CO_2 conversion	H_2/CO ratio
700	71	76	.81	73.6	81.6	.895	-3.66	-7.3	-9.8
750	82	88	.89	84.95	91.65	.924	-3.59	-3.97	-3.8
800	92	95	.95	88.52	94.52	.935	3.8	0.52	1.57

4.2.2 Noble metal catalyst (Rh/Al_2O_3)

The mathematical models for dry reforming of methane have been validated on the basis of percentage methane conversion in FBR1 and MR1. For this purpose, the experimental studies of Prabhu et al. (2000) on methane dry reforming reaction in fixed bed reactor and membrane reactor have been considered. Prabhu et al. (2000) carried out dry reforming in a shell and

भारतीय प्रौद्योगिकी संस्थान रुड़की
श्रमं विना न किमपि साध्यम्
SHRAMAM VINA NA KIMAPI SADHYAM
INDIAN INSTITUTE OF TECHNOLOGY ROORKEE

tube type reactor (4 cm length), dry reforming of methane with carbon dioxide was studied over a 1 wt.% Rh/Al_2O_3catalysThe reactor was operated at atmospheric pressure on both sides. The reactor consisted of two concentric tubes, with the membrane placed in the interior tube, and the packed bed held in the outer annular region (shell side). Experimental results were obtained with a semipermeable Vycor glass membrane. Reaction was carried out in temperature ranging from 848K to 1023K at atmospheric pressure with a total flow rate of 75mols/min of mixed gasses of CH_4:CO_2:Ar=24:24:27. In the present study the, the model equations described in chapter 3 have been solved at same operating conditions as used by Prabhu et al. (2000). Table 4.3 compares the model predictions with experimental results.

Table 4.3
Validation of model results of fixed bed and membrane reactor with experimental results (Prabhu et al. 2000)

Temp(K)	Fixed Bed Reactor		Membrane Reactor		Error (%)	
	Model	Experimental	Model	Experimental	FBR	MR
848	38.04	36.7	41.7	42.7	-3.65	2.34
873	46.37	45.2	50.29	50.3	-2.58	0.02
898	54.91	54.3	59.2	59.9	-1.12	1.16
923	63.16	62.6	64.08	65.3	-0.89	1.86
948	69.8	70.2	72.66	76.1	0.57	4.52
973	77.16	76.8	-	-	-0.46	-

4.3 PERFORMANCE OF FIXED BED REACTOR (FBR1) AND MEMBRANE REACTOR (MR1)

The fixed bed reactor FBR1 and MR1 are reactors packed with noble catalyst Rh/Al_2O_3. The model equations((3.23)-(3.7)) and ((3.10)-(3.15)) given in chapter 3 along with the kinetics equations presented in subsection (3.4.1) and (3.4.2) were solved using tool ODE solver in MATLAB. The boundary conditions, reactor specifications, feed flow rates are presented in the table 3.1. Also the operating temperature, percentage of H_2 in feed and the CO_2/CH_4 feed ratio selected on the basis of thermodynamic analysis are used.

भारतीय प्रौद्योगिकी संस्थान रुड़की
श्रमं विना न किमपि साध्यम्
SHRAMAM VINA NA KIMAPI SADHYAM
INDIAN INSTITUTE OF TECHNOLOGY ROORKEE

4.3.1 Axial Flow Rate Profiles for FBR1 and MR1

Figs (4.14 - 4.16) shows how the molar flow rate of reactants, products and inert varies along the length of the reactor FBR1 and MR1. The reactors are operated at a temperature of 1180K and pressure of 1 atm. For FBR1 as seen from the fig 4.14 we see that as we move along the reactor length the molar flow rate of methane and carbon dioxide decrease continuously, because they are being consumed continuously in reforming reaction and reverse water gas shift (RWGS) reaction. Also, because of the RWGS reaction the conversion of CO_2 is greater than that of methane. If it would not have been for RWGS reaction, the molar flow rate of both CO_2 and CH_4 would had been same. The molar flow rate of products i.e, hydrogen, carbon monoxide and that of water increase along the length of reactor. The molar flow rate of the inert Nitrogen remains constant throughout the length of the reactor. The flow rate of water increases slowly with the length of reactor as it is produced only by RWGS reaction.

For the MR1 in which vycor glass membrane is used, there are two axial flow rate profiles one for the tube side and the other for the shell side of the reactor. Since both the reforming reaction and RWGS reaction are reversible reaction so the removal of one or more products will enhance the reaction and overcomes thermodynamic equilibrium limitations, resulting in increased methane conversion. All the reactants, inert and the products permeate through the membrane towards the shell side as vycor glass membrane is permeable to all the gaseous components. From the fig 4.15 it is noteworthy that for the tube side of MR1 the flow rate profile is almost similar to that obtained in FBR1, only differences being in the flow rate profile of inert nitrogen and the value of flow rates. The molar flow rate of inert nitrogen gas first increases along the length and then attains a constant value. The profile obtained for nitrogen is justified as initially the partial pressure of Nitrogen on the permeate side(shell side) is much higher than that on the reaction side(tube side) of the MR1, so initially the Nitrogen permeates at a higher rate towards the reaction side(tube side), but as the reactions proceed the gaseous species permeate to the shell side thus reducing the partial pressure of Nitrogen on the shell side making the flow rate of Nitrogen almost constant in each side of the MR1. Thus the application of membrane enhances the methane conversion resulting in greater flow rates of products and reduced/lower flow rates of reactants as compared to FBR1.

Fig 4.16 represents the axial profile obtained for the permeate side (shell side) of MR1. The molar flow rate of inert gas nitrogen decreases rapidly first and then attains a value of 0.96μmol/s. The molar flow rates of the three products hydrogen, carbon monoxide and

भारतीय प्रौद्योगिकी संस्थान रुड़की
श्रमं विना न किमपि साध्यम्
SHRAMAM VINA NA KIMAPI SADHYAM
INDIAN INSTITUTE OF TECHNOLOGY ROORKEE

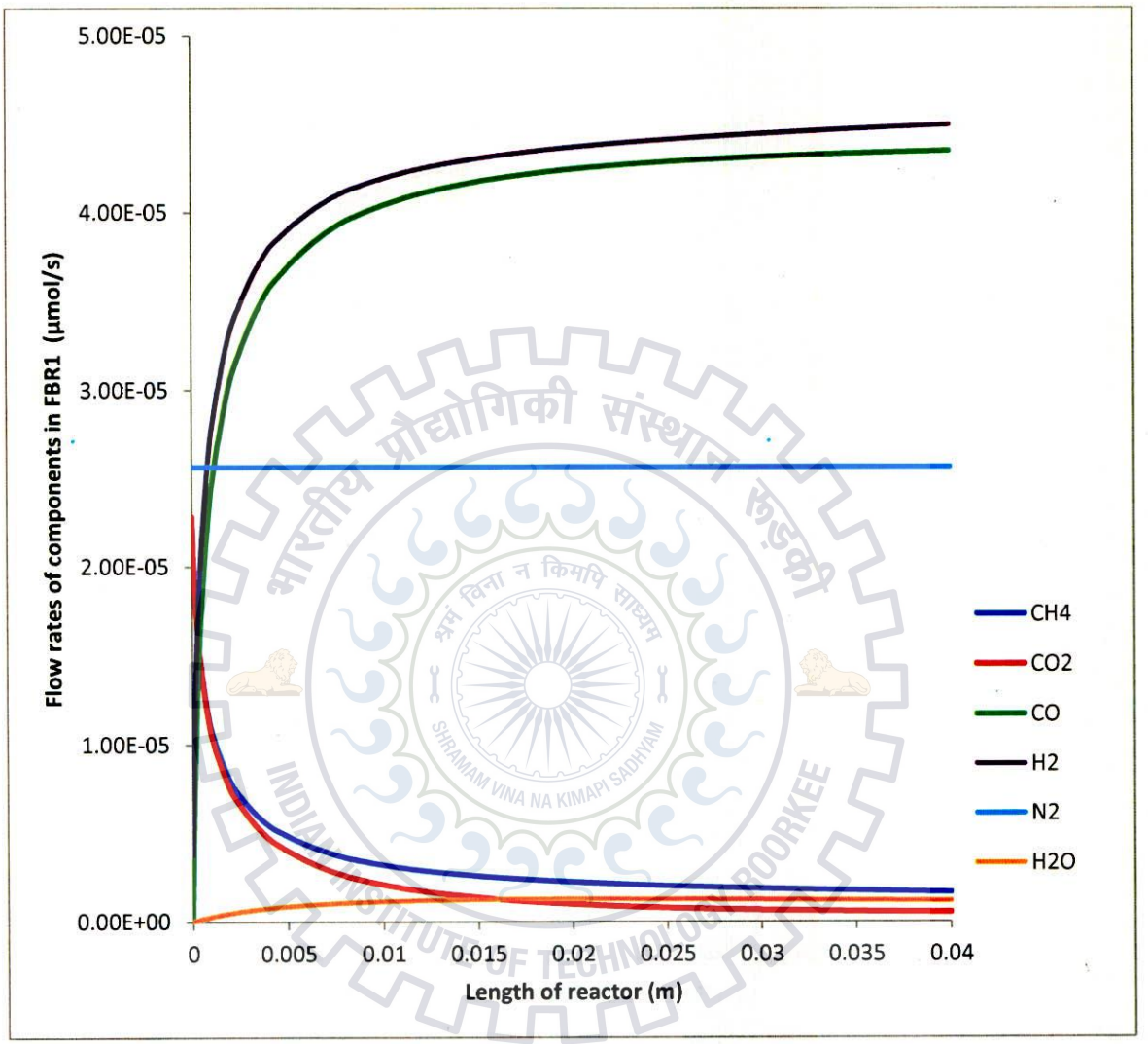

Fig 4.14 Axial variation of flow rates of components in FBR1

भारतीय प्रौद्योगिकी संस्थान रुड़की
श्रमं विना न किमपि साध्यम्
SHRAMAM VINA NA KIMAPI SADHYAM
INDIAN INSTITUTE OF TECHNOLOGY ROORKEE

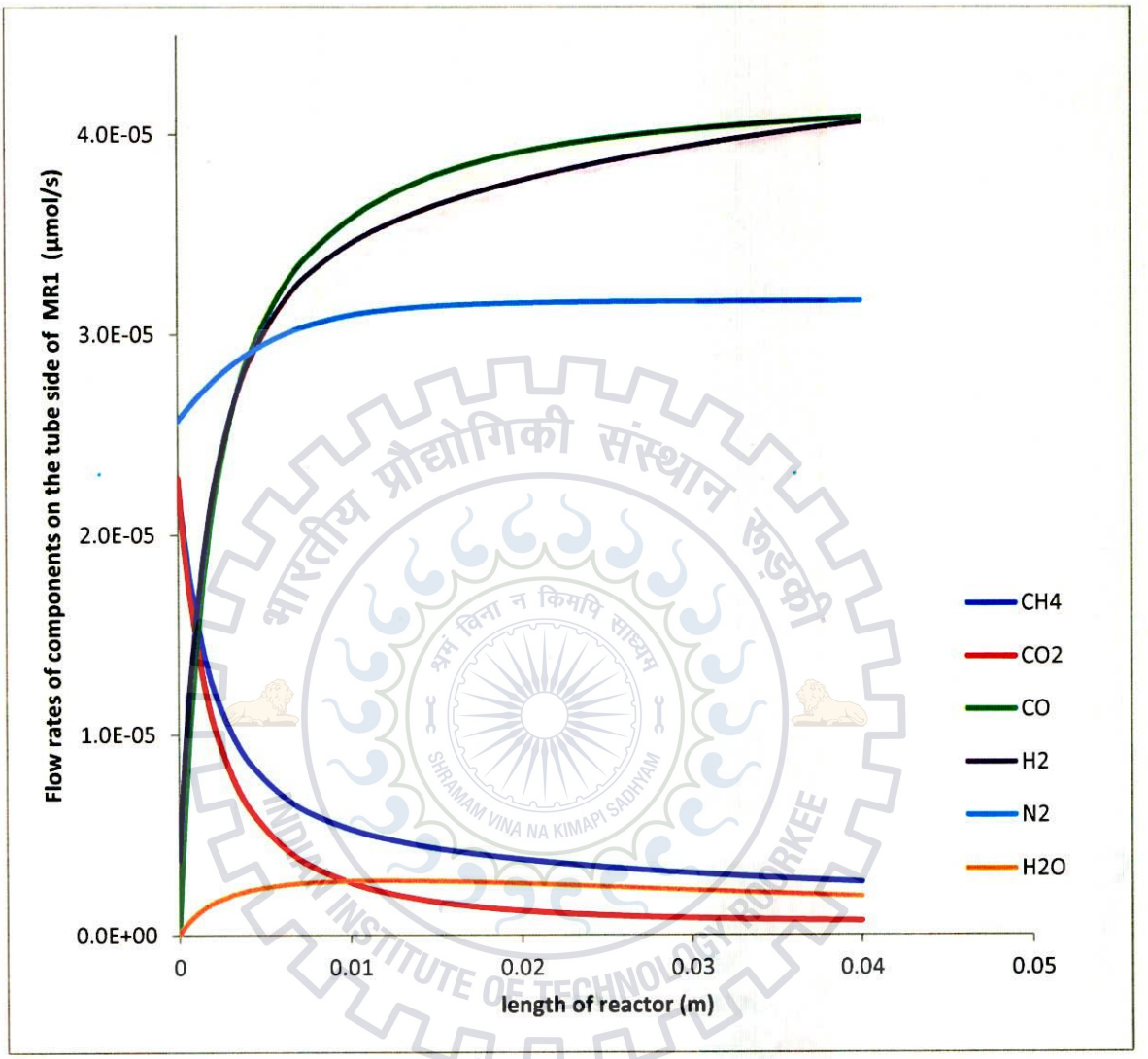

4.15 Axial variation of flow rates of components on tube side of MR1


भारतीय प्रौद्योगिकी संस्थान रुड़की
श्रमं विना न किमपि साध्यम
SHRAMAM VINA NA KIMAPI SADHYAM
INDIAN INSTITUTE OF TECHNOLOGY ROORKEE

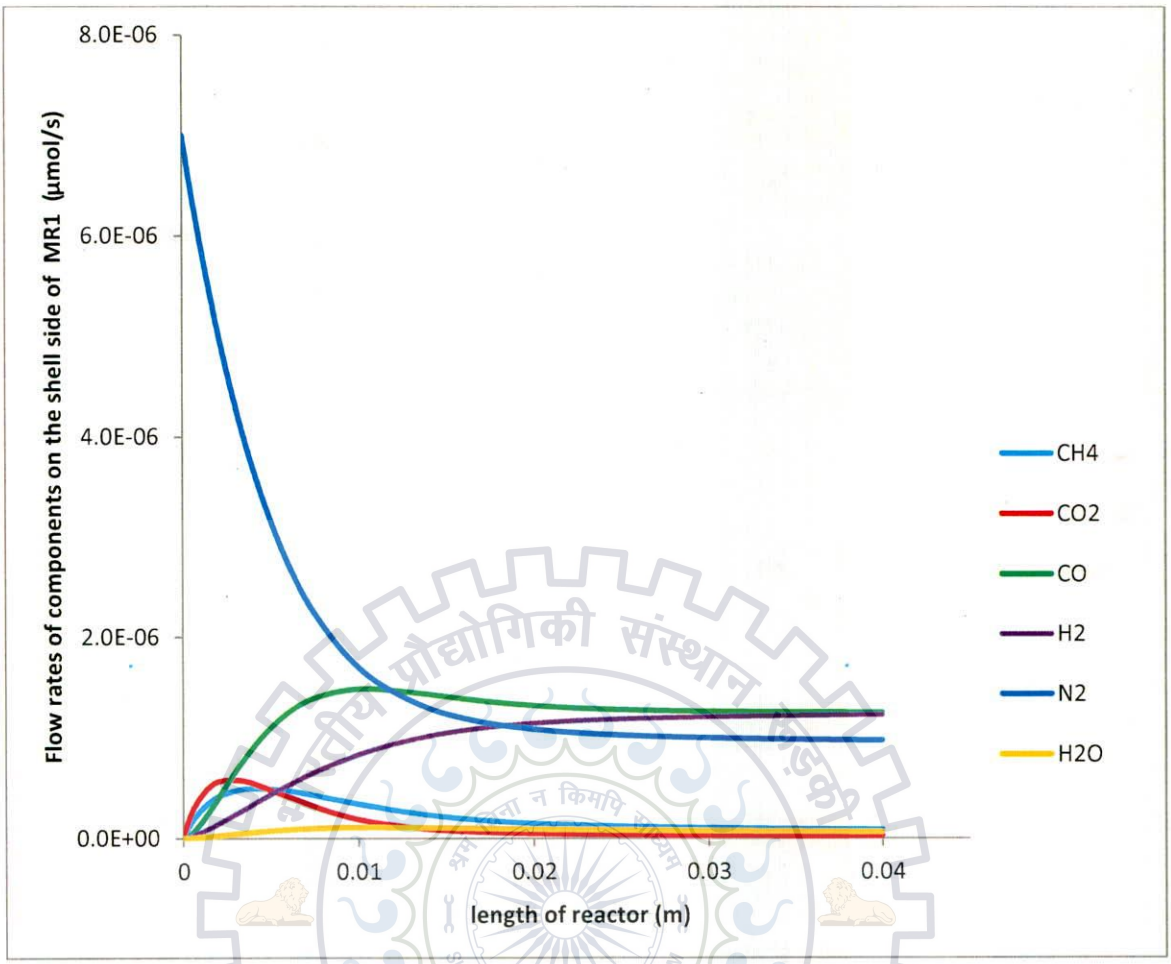

4.16 Axial variation of flow rates of components on shell side of MR1

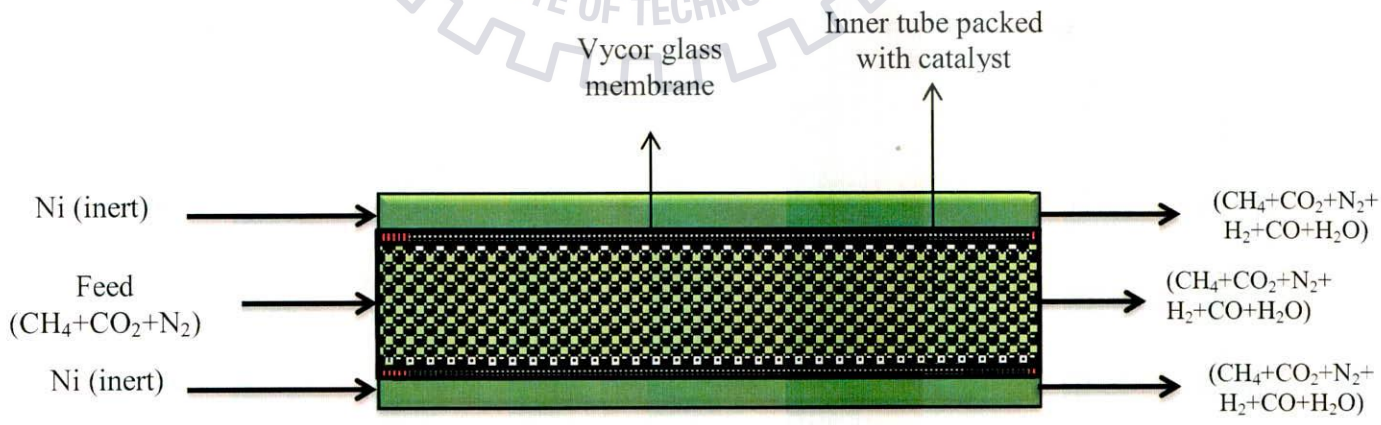

Fig 4.17 Vycor glass membrane reactor


भारतीय प्रौद्योगिकी संस्थान रुड़की
श्रम विना न किमपि साध्यम्
SHRAMAM VINA NA KIMAPI SADHYAM
INDIAN INSTITUTE OF TECHNOLOGY ROORKEE

water increase along the length of the shell side of the reactor. The mechanism for permeation of gaseous species through vycor glass membrane is Knudsen diffusion. As per the Knudsen mechanism the permeability of gaseous component is inversely proportional to the square root of its molecular weight. So on the basis of that the hydrogen molecules should permeate at a greater rate as compared to other two products that are carbon monoxide and water. But hydrogen permeation as seen in the fig 4.16 is less than that of carbon monoxide, the possible reason being that hydrogen is being consumed in RWGS reaction on the tube side (reaction side) and thus its partial pressure difference across the two sides of membrane is lower than that of carbon monoxide, resulting in reduced permeation. The two reactants methane and carbon dioxide are permeated at a greater rate initially as their flow rates are high but as the reactions precede their conversion increases causing decrease of flow rates (thus reduced partial pressures) along the reactor length, thus reducing the permeation of reactants.

Table 4.4
CH_4 conversion, H_2/CO ratio, selectivity and yield at T=1180K, P=1 atm and CO_2/CH_4 =1; (FBR1 &MR1)

Reactor type	H_2 in feed %	% CH_4 conversion	H_2/CO ratio	Selectivity H_2	Yield H_2	Selectivity CO	Yield CO
FBR1	0	97.479	.985	.4939	1.933	.5013	1.9625
	5	97.293	1.0693	.5147	2.096	.4813	1.9605
MR1	0	98.350	.984	.4943	1.9362	.5020	1.9662
	5	98.290	1.0688	.5246	2.186	.4814	1.9614

4.3.2 Axial Flow Rate Profiles for FBR2 and MR2

Figs (4.18 – 4.20) shows how the molar flow rate of reactants, products and inert varies along the length of the reactor FBR2 and MR2. The reactors are operated at a temperature of 1180K and pressure of 1 atm. For FBR2 as seen from the fig 4.18 we can see that as we move along the reactor length the molar flow rate of methane and carbon dioxide decrease continuously, because they are being consumed continuously in reforming reaction and reverse water gas shift(RWGS) reaction. Also, because of the RWGS reaction the conversion of CO_2 is greater than that of methane. If it would not have been for RWGS reaction, the molar flow rate of both CO_2 and CH_4 would had been same. The molar flow rate of products i.e, hydrogen,

भारतीय प्रौद्योगिकी संस्थान रुड़की
श्रमं विना न किमपि साध्यम्
SHRAMAM VINA NA KIMAPI SADHYAM
INDIAN INSTITUTE OF TECHNOLOGY ROORKEE

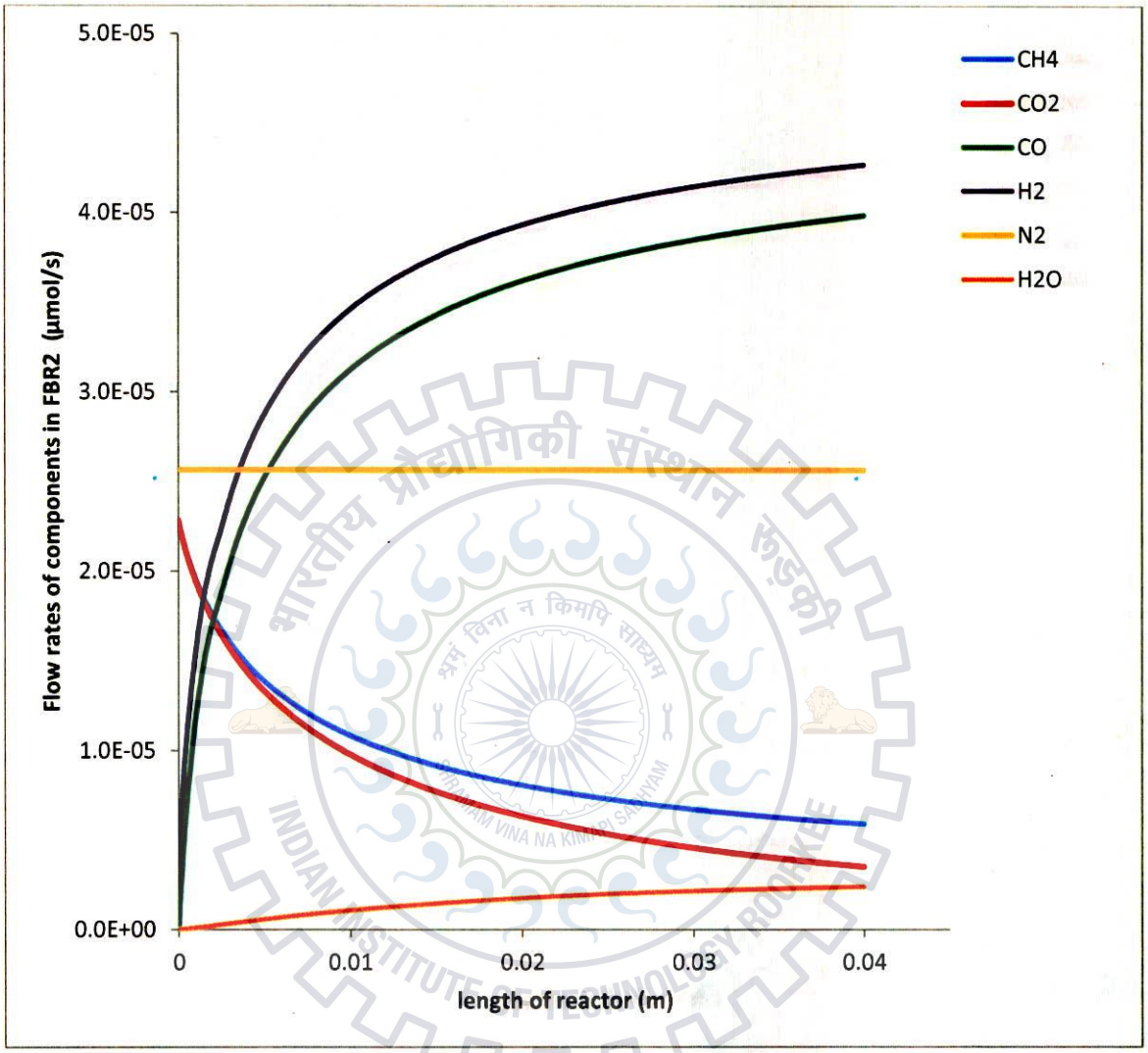

Fig 4.18 Axial variation of flow rates of components in FBR2


भारतीय प्रौद्योगिकी संस्थान रुड़की
श्रमं विना न किमपि साध्यम्
SHRAMAM VINA NA KIMAPI SADHYAM
INDIAN INSTITUTE OF TECHNOLOGY ROORKEE

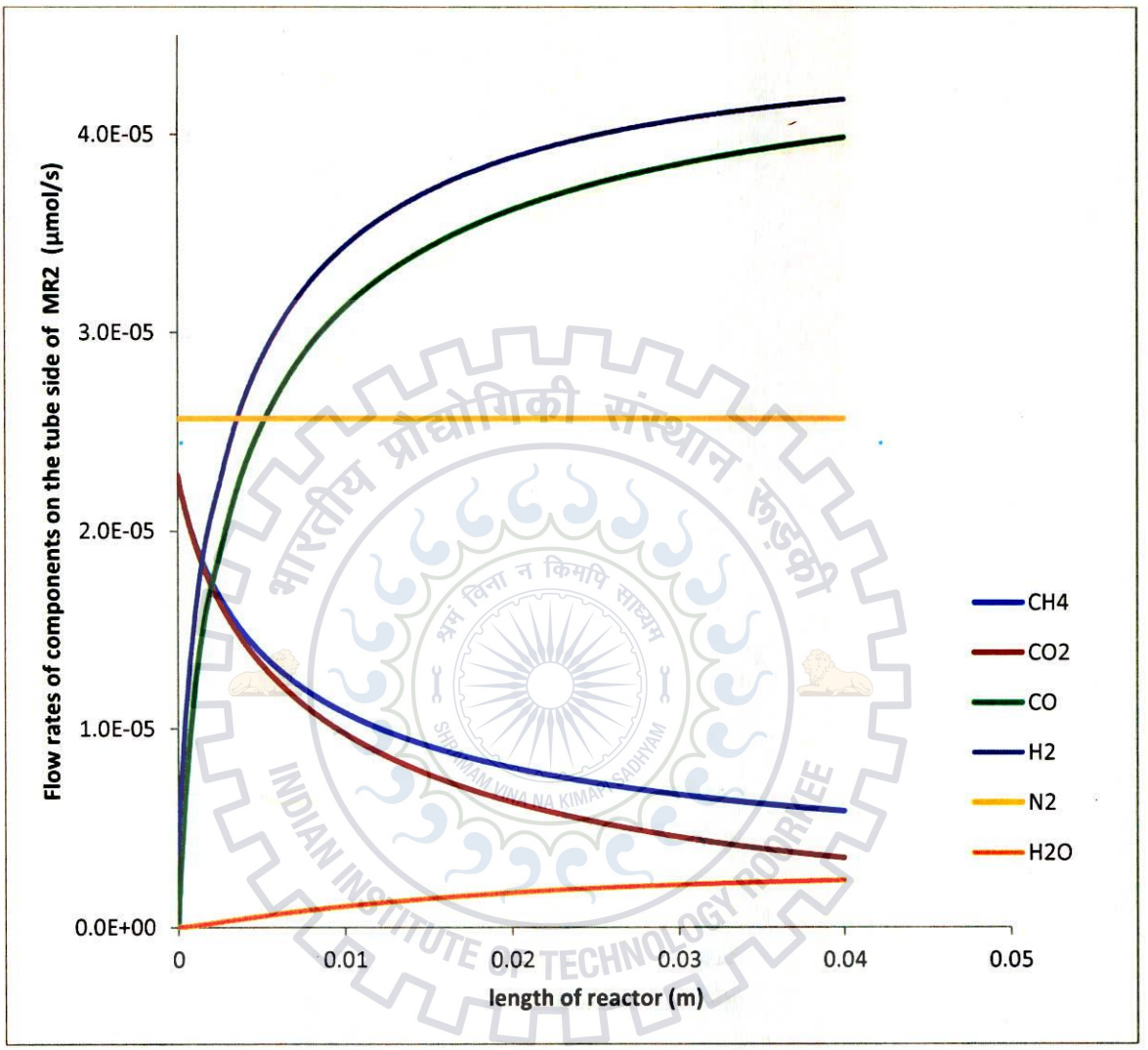

Fig 4.19 Axial variation of flow rates of components on tube side of MR2


भारतीय प्रौद्योगिकी संस्थान रुड़की
श्रमं विना न किमपि साध्यम्
SHRAMAM VINA NA KIMAPI SADHYAM
INDIAN INSTITUTE OF TECHNOLOGY ROORKEE

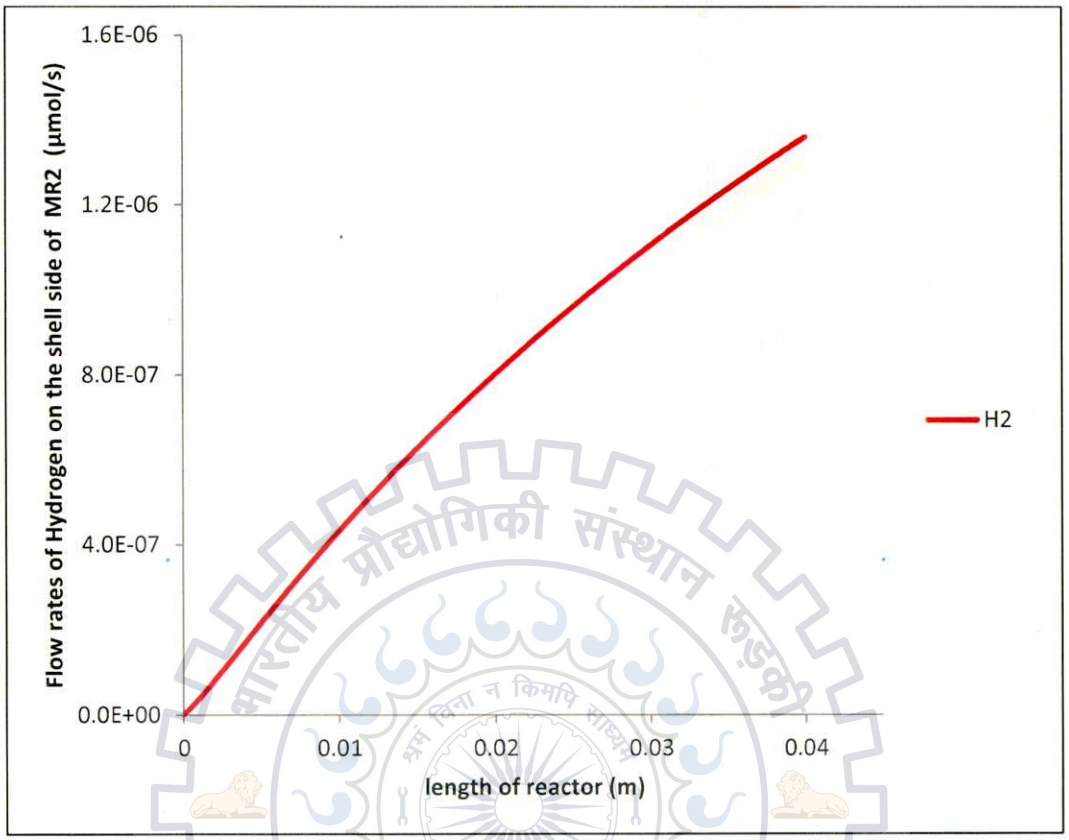

Fig 4.20 Axial variation of flow rates of hydrogen on shell side of MR2

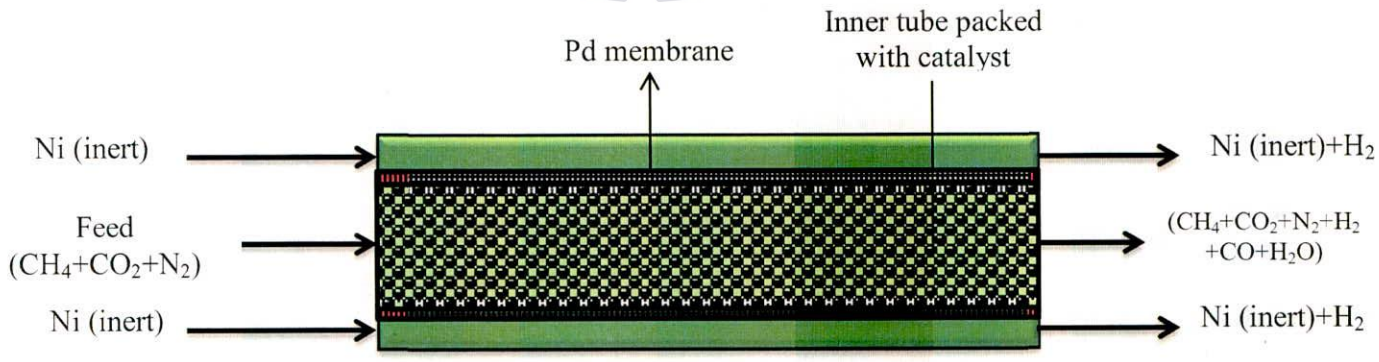

Fig 4.21 Pd dense membrane reactor packed with Ni/Al_2O_3


भारतीय प्रौद्योगिकी संस्थान रुड़की
श्रमं विना न किमपि साध्यम्
SHRAMAM VINA NA KIMAPI SADHYAM
INDIAN INSTITUTE OF TECHNOLOGY ROORKEE

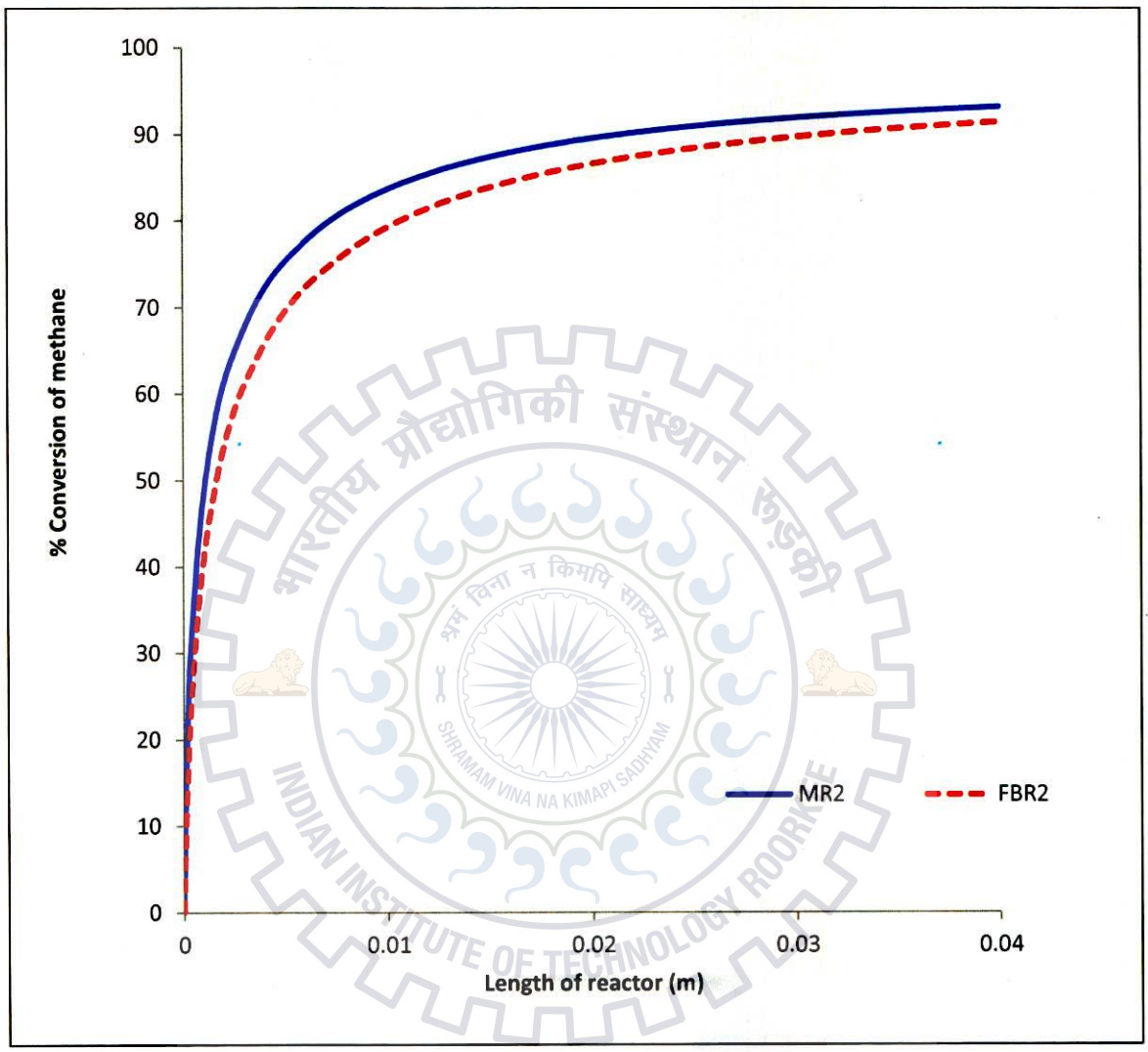

Fig 4.22 Axial variation of percent conversion of methane in MR2 and FBR2.

भारतीय प्रौद्योगिकी संस्थान रुड़की
श्रम विना न किमपि साध्यम्
SHRAMAM VINA NA KIMAPI SADHYAM
INDIAN INSTITUTE OF TECHNOLOGY ROORKEE

carbon monoxide and that of water increase along the length of reactor. The molar flow rate of the inert Nitrogen remains constant throughout the length of the reactor. The flow rate of water increases slowly with the length of reactor as it is produced only by RWGS reaction. It is noteworthy from the fig…that the flow-rates do not attain a constant value, which means that equilibrium is not attained for the given length of reactor.

For the MR2 in which dense Pd membrane has been used, there are two axial flow rate profiles one for the tube side and the other for the shell side of the reactor. Since both the reforming reaction and RWGS reaction are reversible reaction so the removal of one or more products will enhance the reaction and overcomes thermodynamic equilibrium limitations, resulting in increased methane conversion. Hydrogen permeates through the membrane towards the shell side as Pd-dense membrane is permeable to only this component. From the fig 4.19 it is noteworthy that for the tube side of MR2 the flow rate profile is almost similar to that obtained in FBR1, only differences being in the values of flow rates. Unlike in MR1 the molar flow rate of inert nitrogen on the tube side remains constant along the length of the reactor.

Fig 4.20 represents the axial profile obtained for the permeate side (shell side) of MR2. The molar flow rate of inert gas nitrogen remains constant throughout the reactor length at a value of 7μm/s. The molar flow rates of the only permeated product, hydrogen increases along the length of the shell side of the reactor.

From the results presented in table 4.5 it is noteworthy that the application of membrane enhances the methane conversion resulting in greater flow rates of products and reduced/lower flow rates of reactants as compared to FBR2.

Table 4.5
CH_4 conversion, H_2/CO ratio, selectivity and yield at T=1180K, P=1 atm and CO_2/CH_4 =1; (FBR2 & MR2)

Reactor type	H_2 in feed %	% CH_4 conversion	H_2/CO ratio	Selectivity H_2	Yield H_2	Selectivity CO	Yield CO
FBR2	0	90.72	.9577	.4839	1.84	.5053	1.9212
	5	91.29	1.039	.5039	1.993	.4848	1.9175
MR2	0	94.125	.9586	.4843	1.807	.5052	1.9225
	5	93.77	1.0405	.5150	1.996	.4950	1.9188

भारतीय प्रौद्योगिकी संस्थान रुड़की
श्रमं विना न किमपि साध्यम्
SHRAMAM VINA NA KIMAPI SADHYAM
INDIAN INSTITUTE OF TECHNOLOGY ROORKEE

10. Haag Stéphane, Michel Burgard, Barbara Ernst , "**Beneficial effects of the use of a nickel membrane reactor for the dry reforming of methane: Comparison with thermodynamic predictions**", Journal of Catalysis 252 (2007) 190–204

11. http://en.wikipedia.org

12. Huang Tao, Wei Huang, Jian Huang, Peng Ji "**Methane reforming reaction with carbon dioxide over SBA-15 supported Ni–Mo bimetallic catalysts",** Fuel Processing Technology 92 (2011) 1868–1875

13. Intergovernmental Panel on Climate Change, Climate Change 2001: The Scientific Basis (Eds.: J. T. Houghton, Y. Ding, D. J. Griggs, M. Noguer, P. J. van der Linden, X. Dai, K. Maskell, and C. A. Johnson), Cambridge University Press, Cambridge, 2001.

14. J. Múnera, S. Irusta, L. Cornaglia, E. Lombardo, "**CO_2 reforming of methane as a source of hydrogen using a membrane reactor",** Applied Catalysis A: General 245 (2003) 383–395.

15. Kang Ki-Moon , Hyo-Won Kim, Il-Wun Shim, Ho-Young Kwak **"Catalytic test of supported Ni catalysts with core/shell structure for dry reforming of methane**", Fuel Processing Technology Volume 92, Issue 6, June 2011, Pages 1236–1243.

16. Kumar Shashi, Mohit Agrawal, Surendra Kumar, Sheeba Jilan, "**The Production of Syngas by Dry Reforming in Membrane Reactor Using Alumina-Supported Rh Catalyst:A Simulation Study**" International journal of Chemical Reactor Engineering, 6, 1-37(2008).

17. Liu Dapeng, Yifan Wang, Daming Shi , Xinli Jia , Xin Wanga, Armando Borgna , Raymond Lau, Yanhui Yang, "**Methane reforming with carbon dioxide over a Ni/ZiO_2-SiO_2 catalyst: Influence of pretreatment gas atmospheres**", International journal of hydrogen energy 37 (2012) 10135-10144.

18. Nikoo Khoshtinat M., N.A.S. Amin "**Thermodynamic analysis of carbon dioxide reforming of methane in view of solid carbon formation**", Fuel Processing Technology 92 (2011) 678–691.

19. Nowosielska M., W.K. Jozwiak, J. Rynkowski "**Reforming of methane with carbon dioxide over supported bimetallic catalysts containing Ni and noble metal I. Characterization and activity of SiO_2 supported Ni–Rh catalysts**" Applied Catalysis A: General 280 (2005) 233–244.

20. Pawelec A. , S. Damyanova ,K. Arishtirova, J.L.G. Fierro,L., Petrov, **"Structural and surface features of Pt-Ni catalysts for reforming of methane with CO_2"** Applied Catalysis A: General Volume 323, 30 April 2007, Pages 188–201.


भारतीय प्रौद्योगिकी संस्थान रुड़की
श्रमं विना न किमपि साध्यम
SHRAMAM VINA NA KIMAPI SADHYAM
INDIAN INSTITUTE OF TECHNOLOGY ROORKEE

21. Pinheiro A.N., A. Valentini, J.M. Sasaki, A. C. Oliveira **"Structural characterization of highly stable Pt–Ni supported zeolites and its catalytic performance for methane reforming with CO_2 "** Studies in Surface Science and Catalysis Volume 174, PartA, 2008, Pages 205–208.

22. Prabhu A.K., A. Liu, L.G. Lovell, S.T. Oyama, **"Modeling of the methane reforming reaction in hydrogen selective membrane reactors"**, Journal of Membrane Science 177 (2000) 83–95.

23. Richardson, J.T., and S.A. Paripatyadar, "**Carbon dioxide reforming of methane with supported Rhodium**", Appl. Catalysis, 61, 293-309 (1990).

24. Sokolov Sergey, Evgenii V. Kondratenko, Marga-Martina Pohl, Axel Barkschat, Uwe Rodemerck **"Stable low-temperature dry reforming of methane over mesoporous La2O3-ZrO2 supported Ni catalyst"**, Applied Catalysis B: Environmental 113– 114 (2012) 19– 30

25. Soria M.A., C.Mateos-Pedrero, A.Guerrero-Ruiz, Rodríguez-Ramos **"Thermodynamic and experimental study of combined dry and steam reforming of methane on Ru/ ZrO_2-La_2O_3 catalyst at low temperature"** International Journal of Hydrogen Energy Volume 36, Issue 23 (2011) 15212-15220.

26. Sun Y.., T. Ritchie, S. S. Hla, S.McEvoy, W. Stein, J. H. Edwards. **"Thermodynamic analysis of mixed and dry reforming of methane for solar thermal applications"**, Journal of Natural Gas Chemistry 20(2011)568–576.

27. Teddy G. Monroya, Leonila C. Abellaa, Susan M. Gallardoa, Hirofumi Hinode **"Catalytic Dry Reforming of Methane Using Ni/MgO-ZrO_2 Catalyst"**, Proceedings of the 2nd Annual Gas Processing Symposium 2010, Pages 145–152.

28. Tu X., J.C. Whitehead **"Plasma catalytic dry reforming of methane in an atmospheric dielectric barrier discharge: Understanding the synergistic effect at low temperature"** Applied Catalysis B: Environmental Volume 125, 21 August 2012, Pages 439–448.

29. Wang H.Y., C.T. Au, **"Carbon dioxide reforming of methane to syngas over SiO_2-supported rhodium catalysts"**, Applied Catalysis A: General 155 (1997) 239-252.

30. Wang Shaobin, G.Q. Lu, **"Reforming of methane with carbon dioxide over Ni/Al_2O_3 catalysts: Effect of nickel precursor"**, Applied Catalysis A: General 169 (1998) 271-280.

भारतीय प्रौद्योगिकी संस्थान रुड़की
श्रमं विना न किमपि साध्यम्
SHRAMAM VINA NA KIMAPI SADHYAM
INDIAN INSTITUTE OF TECHNOLOGY ROORKEE

Fig 4.21 shows methane conversion profiles in the axial direction at a temperature of 1180K. From the figure it can be noted that as the length of the reactor increases the conversion of CH_4 also increases. But the conversions attained are not the equilibrium conversions, so the length of the reactor that is 0.04m is not the sufficient length to attain equilibrium conversions. The conversion of the methane at the exit of the membrane reactor (93.77%) is higher than that of that achieved in fixed bed reactor(91.29%) at 1180K.


भारतीय प्रौद्योगिकी संस्थान रुड़की
श्रम विना न किमपि साध्यम्
SHRAMAM VINA NA KIMAPI SADHYAM
INDIAN INSTITUTE OF TECHNOLOGY ROORKEE

CONCLUSIONS

Thermodynamic study of carbon dioxide reforming of methane was carried out using Gibbs free energy minimization approach. Four carbon formation reactions: methane cracking, boudard reaction, CO reduction reaction, and CO_2 reduction were considered. Equilibrium conversion of the reactants, product composition and carbon formation was influenced by the reaction temperature and the feed CO_2/CH_4 ratio. The feed ratio was varied from 1 to 3 and temperature range from 873-1500K and its effect on the methane conversion, carbon dioxide conversion, carbon formation, H_2 yield, H_2 selectivity, H_2/CO ratio and CO selectivity was studied. Also, the effect of addition of H_2 in the feed has been studied. The percentage of H_2 in the feed has been varied from 0 to 10%. The addition of H_2 resulted in the reduction of carbon formation and at the same time increases the yield and selectivity of Hydrogen. Thermodynamic analysis revealed that the optimal working conditions for syngas(H_2/CO=1) production are, a temperatures of about 1180 K, 5% H_2 addition in feed and CO_2/CH_4 ratio of 1 at which about 4 mol of syngas could be produced from 2 mol of reactants with negligible amount of carbon formation.

The operating conditions obtained from thermodynamic analysis have been used to analyse the performance of different reactors used for DRM. For that one dimensional, steady state, isothermal mathematical model incorporating the kinetics for Rh/Al_2O_3 and Ni/Al_2O_3 catalyst for the carbon dioxide reforming of methane was developed. The model was developed to analyse the performance of four different reactors, two fixed bed reactors [FBR1(Rh/Al_2O_3) & FBR2(Ni/Al_2O_3)] and two membrane reactors [MR1(Rh/Al_2O_3, vycor glass membrane) & MR2(Ni/Al_2O_3, Pd membrane)]. The reactors were analysed in terms of methane conversion, H_2/CO ratio, yield and selectivity of H_2 and CO. The simulation study of the reactors showed that in both cases at 1180K the methane conversion was higher in membrane reactors than that in fixed bed reactor, as the products were continuously being removed from the reaction (tube side) zone of the membrane reactors.

The addition of 5% H_2 in the feed increases the yield of H_2 resulting in greater yield than that of CO for all the four reactor configurations. This makes the H_2/CO ratio slightly greater than 1, thus making it fit for the use in Fisher Tropsch syntheses. Also the selectivity of H_2 also increased on addition of 5% H_2 in the feed. At the optimum condition, H_2/CO ratio was maintained in unity and water formation minimized.


भारतीय प्रौद्योगिकी संस्थान रुड़की
श्रम विना न किमपि साध्यम्
SHRAMAM VINA NA KIMAPI SADHYAM
INDIAN INSTITUTE OF TECHNOLOGY ROORKEE

Greater conversions were obtained for the reactors (FBR1 & MR1) packed with Rh/Al_2O_3 catalyst as compared to that obtained for reactors(FBR2 & MR2) packed with Ni/Al_2O_3. The methane conversion increased in the order FBR2<MR2<FBR2<MR2. For the given dimensions of the reactors the close to equilibrium values of conversion, yield, and selectivity and H_2/CO ratio are achieved rapidly in reactors employing Rh/Al_2O_3 catalyst.

Recommendations

In future, the models can be modified to consider non-isothermal conditions, effects of pressure drop or fluid dynamic, the effectiveness factor as well as coking rate on the reactor performances. Also coupling exothermic reaction of methane oxidation with the endothermic CO_2 reforming of methane could be considered as it reduce the energy requirements and also control the thermal behaviour of the reaction system.


भारतीय प्रौद्योगिकी संस्थान रुड़की
श्रमं विना न किमपि साध्यम
SHRAMAM VINA NA KIMAPI SADHYAM
INDIAN INSTITUTE OF TECHNOLOGY ROORKEE

REFRENCES

1. Al-Fatesh Ahmed S. A., Anis H. Fakeeha and Ahmed E. Abasaeed "**Effects of promoters on methane dry reforming over Ni catalyst on a mixed (a-Al_2O_3+TiO_2-P25) support**", International Journal of the Physical Sciences 36, (2011) 8083 – 8092.

2. Amin Nor Aishah Saidina, Tung Chun Yaw "**Thermodynamic equilibrium analysis of combined carbon dioxide reforming with partial oxidation of methane to syngas**", International Journal of Hydrogen Energy 32 (2007) 1789 – 1798.

3. Becerra Alberto M., María E. Iriarte and Adolfo E. Castro-Luna, "**Catalytic Activity of a Nickel on Alumina Catalyst in The CO_2 Reforming Of Methane**", React.Kinet.Catal. 79, (2003) 1119-1125

4. Benrabaa R., A. Lofberg, A. Rubbens, E. Bordes-Richard, R.N. Vannier, A. Barama, **"Structure, reactivity and catalytic properties of nanoparticles of nickel ferrite in the dry reforming of methane"**, Catalysis Today 203, 30 March 2013, Pages 188–198.

5. Bosko M.L., J.F. Múnera, E.A. Lombardo, L.M. Cornaglia "**Dry reforming of methane in membrane reactors using Pd and Pd–Ag composite membranes on a NaA zeolite modified porous stainless steel support**", Journal of Membrane Science 364 (2010) 17–26.

6. Demidov D.V. , I.V. Mishin , M.N. Mikhailov "**Gibbs free energy minimization as a way to optimize the combined steam and carbon dioxide reforming of methane**", International journal of hydrogen energy 36 (2011) 5941-5950.

7. Erhan A. Aksoylu ,Seyma Ozkara-Aydınoglu, **"CO_2 reforming of methane over Pt-Ni/Al_2O_3 catalysts: Effects of catalyst composition, and water and oxygen addition to the feed"** international journal of hydrogen energy 36 (2011) 2950-2959.

8. Gallucci F., S. Tosti b, A. Basile, "**Pd–Ag tubular membrane reactors for methane dry reforming: A reactive method for CO_2 consumption and H_2 production**" Journal of Membrane Science 317 (2008) 96–105.

9. Gamba Oscar, Sonia Moreno, Rafael Molina "**Catalytic performance of Ni-Pr supported on delaminated clay in the dry reforming of methane",** International journal of hydrogen energy 36 (2011) 1540-1550.


भारतीय प्रौद्योगिकी संस्थान रुड़की
श्रमं विना न किमपि साध्यम्
SHRAMAM VINA NA KIMAPI SADHYAM
INDIAN INSTITUTE OF TECHNOLOGY ROORKEE

31. Xu Junke, Wei Zhou, Jihui Wang ,Zhaojing LI ,Jianxin Ma, **"Characterization and Analysis of Carbon Deposited during the Dry Reforming of Methane over $Ni/La_2O_3/Al_2O_3$ Catalysts",** Chinese Journal of Catalysis Volume 30, Issue 11, November 2009, Pages 1076–1084

32. Yanbing Li, Jin Baosheng and Xiao Rui "**Carbon dioxide reforming of methane with a free energy minimization approach**", Korean J. Chem. Eng., 24(4), 688-692 (2007).

33. Zebao Rui a, Hongbing Ji , Y.S. Lin b, "**Modelling and analysis of ceramic carbonate dual-phase membrane reactor for carbon dioxide reforming with methane**", International journal of hydrogen energy 36 (2011) 8292-8300.

34. Zhang Jianguo, Hui Wang, and Ajay K. Dalai , "**Kinetic Studies of Carbon Dioxide Reforming of Methane over Ni-Co/Al-Mg-O Bimetallic Catalyst**", Ind. Eng. Chem. Res. 2009, 48, 677–684.

35. Quiroga Marı´a Martha Barroso, Adolfo Eduardo Castro-Luna, **"Catalytic activity and effect of modifiers on Ni-based catalysts for the dry reforming of methane",** International journal of hydrogen energy 35 (2010) 6052-6056.